Chapter 1
Introduction and literature review

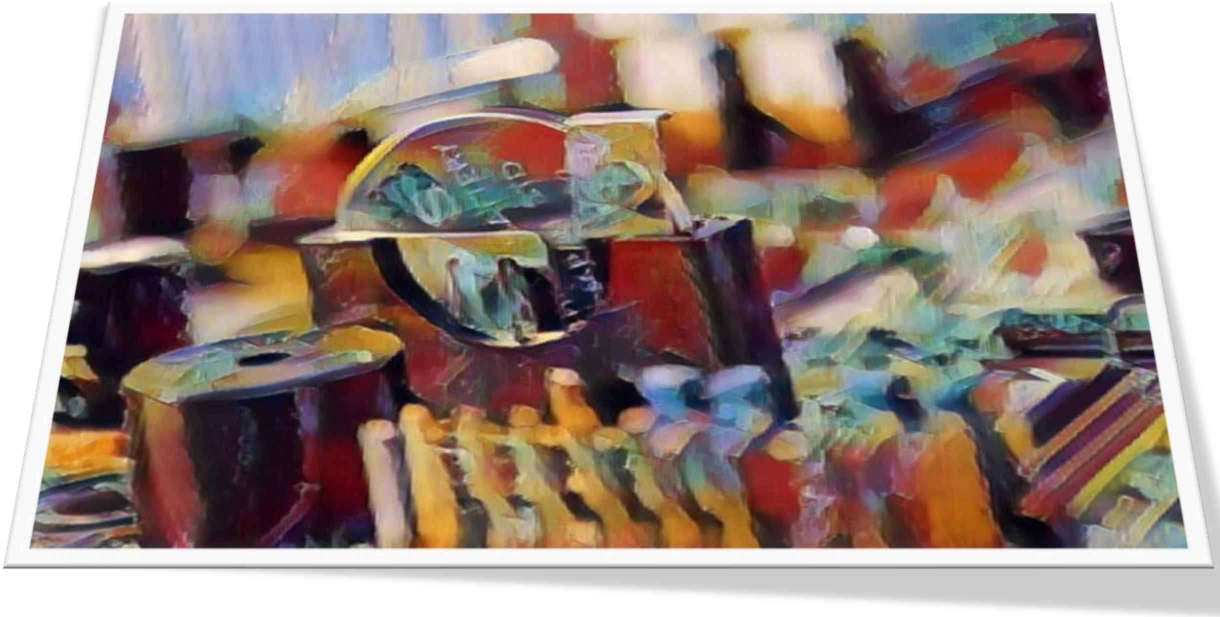

Chapter 1: Introduction and literature review

The prediction by expert regarding the energy market to grow 2.5 to 4 terawatt hours (TWh) each year by 2030, approximately 3 to 5 times the current scenario of growth 800-GWh of the energy market, according to the US Department of Energy's (DOE's) latest reports [1]. The demand for efficient storage encourages researchers to develop device by synthesizing the new materials. The main electrical energy storage devices are batteries, capacitors, fuel cells, and solid-state film capacitors [1]. These devices can be divided into two categories based on performance, long-term storage, and short-term storage devices [1,13]. The energy storage devices' performance is usually measured in terms of two essential parameters: energy density and power density. In order to store energy for long periods of time, batteries use electrochemical reactions to turn chemical energy into electrical energy. Their energy density is between 10 and 300 Wh/kg, while their power density is less than 500 W/kg [1,13]. Batteries are excellent for big and steady energy supply applications because to their performance. Capacitors, on the other hand, are short-term energy storage devices that store energy by physical charge separation between two electrodes [1,13,14]. Dielectric capacitors can supply up to 108 W/kg of capacitance, making them perfect for high-power applications like electric automobiles (<30Wh/kg). Traditional dielectric capacitors use dielectric polymers or ceramics with a density of 102-101 Wh/kg (less than 2 J/cm^3) [13,14]. It is not possible to meet the power density needs of certain ultra-high-power electronics and systems using electrochemical supercapacitors, unlike standard dielectric capacitors, despite their moderate energy density. To make matters worse, the high leakage current and low cycle lift of electrochemical supercapacitors prevent them from being used in some modern pulsed power systems. Supercapacitors have a convoluted physical structure with a low (~ 3.0 V) limited maximum operating voltage (and a low cycling lift of just 10^5) [15]. Dielectric capacitors might potentially compete with electrochemical supercapacitors and even batteries if their energy storage density could be increased [16]. Dielectric capacitors having high energy storage densities may enable smaller, lighter, and more integrated electronic and electrical systems [17]. Higher energy density may be achieved using polymer-based nanocomposite dielectric materials because of their high working voltages. Polymer based ferroelectric material having high dielectric breakdown strength and high electric displacement or polarization is expected to be more promising in this area [2,6]. Capacitors are categorized depending on their energy density and power storage capacity as shown in the Figure 1.1. PVDF based capacitors are promising as they have high power density with moderately high energy density.

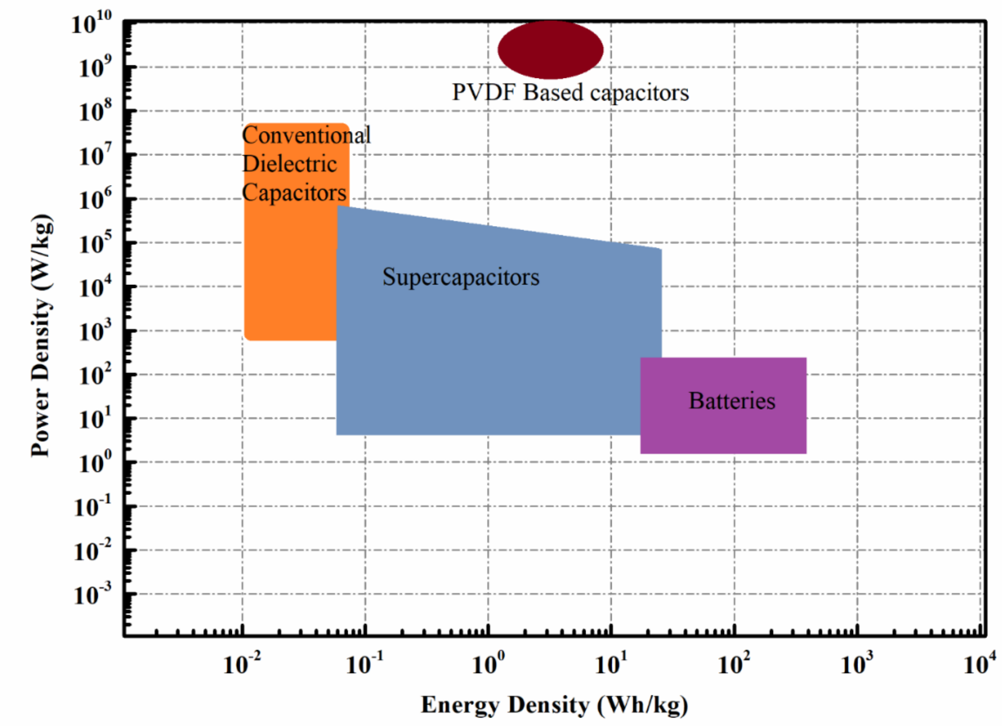

Figure 1.1 Categorization of the storage device according to energy and power.

1.1 Dielectric and Ferroelectric materials

Dielectric materials are generally electric insulators which can become polarized when an external electric field is applied [2,17]. To describe the level of charges that have been induced or switched, commonly known as the polarized level, equation introduces polarization (P). It is defined as the displacement of the charge that is not free to move and attached to the nucleus (bound charge) or the orientation of dipoles per unit volume in response to the applied electric field E_{ext} [18].

$$E = E_{ext} - E_i \tag{1.1}$$

Permittivity (ε), a measurement that reveals how rapidly a dielectric material may become polarized in response to an applied electric field, can help in understanding how the electrostatic field or flux is created in dielectrics per unit charge[19]. This is done by using the permittivity/dielectric constant measurement. Electric displacement is a term that is used to represent the total surface charge density that has been caused by an external field [20–22].

$$D = \varepsilon_0 E + P \tag{1.2}$$

$$P = \chi \, \varepsilon_0 E \tag{1.3}$$

Where D is the electric displacement and ε_0 is dielectric constant of free space.

$$D = \varepsilon_0 E + \chi \, \varepsilon_0 E = \varepsilon_r \varepsilon_0 E = \varepsilon E \tag{1.4}$$

$$\varepsilon = \frac{D}{E} \tag{1.5}$$

ε_r is the dielectric constant of the material.

A sinusoidal voltage applied to an ideal dielectric will create a charging current. When alternating voltage is applied to a dielectric, the current direction changes every half cycle, altering the direction of the polarization [20–22]. So, the mechanisms of materials getting polarized are studied in order to have a better understanding of the dielectric characteristics of materials. ionic polarization, Space charge polarization (Interfacial polarization), dipolar polarization, and electronic polarization are the four categories into which polarization mechanisms can be divided. The applied electric field on the material affects the induced dipole moment in a electroactive material. The relationship between induced dipole moments and the electric field is established using a concept known as polarizability [21,22].

$$P = \alpha E \tag{1.6}$$

The contribution of the different polarization mechanism and the average dipole moment per molecule can be given by

$$P_{av} = \alpha_e E_{loc} + \alpha_i E_{loc} + \alpha_d E_{loc} \tag{1.7}$$

where α_e, α_i, α_d, are electronic, ionic and dipolar polarizability and E_{loc} is local field which defined as

$$E_{loc} = E + \frac{1}{3\varepsilon_0} P \tag{1.8}$$

Interfacial polarization is not added to the average polarization, it can be understand as the interface polarization occurs at the interfaces which can't be added to the typical polarization per molecule of the bulk materials [21,22]. Further, local fields of the interfaces have not been clearly understood yet.

The detailed discussion on the types of polarization is done further as follow:

1.1.1 Space charge (Interfacial) Polarization

Interfacial polarization or space charge polarization occurs due to the accumulation of charge at the boundary between two materials having different conductivities or fermi levels. The charge carriers like ions, electrons, and holes may be trapped at the boundary between two phases or in crystal defects and impurities inside the nanocomposite. In this scenario, space charges will emerge, affecting the average dielectric constant and total polarization [21]. Figure 1.2 illustrates the two ways that interfacial polarization could occur. Accumulation of charge carriers at the boundary between two phases can be understood with the help of Figure 1.2. Charge carriers are trapped (left) at defects (right) that cause interfacial polarisation. In nanocomposite materials at the frequency of 1kHz, space charge polarization plays important role to achieve the desired dielectric properties in nanocomposites.

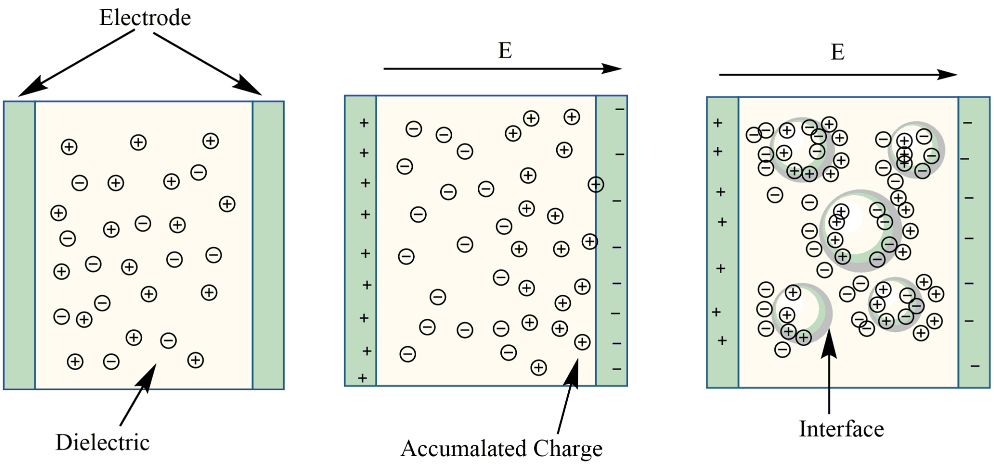

Figure 1.2 Schematic diagram of space charge polarization in a capacitor

1.1.2 Dipolar polarization

Materials having permanent dipole moment have dipolar polarization in the molecules. The best illustration of this is liquid water, where each molecule is a tiny dipole that may be oriented in any direction relative to the other molecule [21-22]. PVDF-based ferroelectric polymers also have dipolar polarization in its molecule as it has permanent dipole moment. Figure 1.3 depicts PVDF's polar phase. Permanent dipoles are oriented C-F bonds. phase spontaneously polarises dipoles. Dipolar polarisation is bigger than atomic and electronic. Ferroelectric materials spontaneously shift and polarise nonlinearly. Due to considerable displacement, dipolar polarisation dominates ferroelectric permittivity.

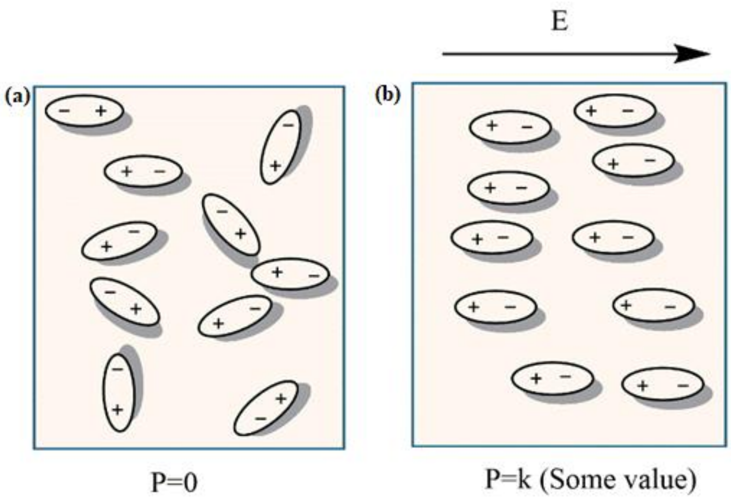

Figure 1.3 Schematic diagram of the dipole orientation (a) without applied field and (b) with applied field.

1.1.3 Ionic polarization

Positive and negative ions in an ionic crystal are moved apart in a manner that causes ionic polarisation. When there are multiple types of atoms in a crystal or molecule, the distribution of charges surrounding each atom tends to be positive or negative. The figure 1.4 shows the Ionic polarization inside the crystal. When there is no electric field applied to the solid then there is not net polarization. In this situation, the effects of dipole moments of equal magnitude are neutralised. Further, the material is connected to the voltage then there will be suitable electric field depending on the thickness of the sample so the positive and negative ions are pushed in opposite direction to each other that causes the net polarization. The electric field affects this polarization's intensity.

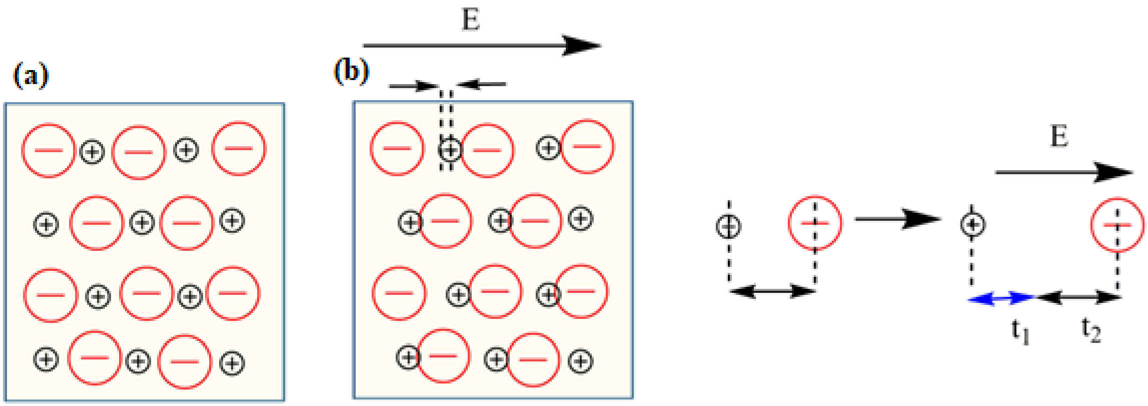

Figure 1.4 Schematic diagram of Ionic polarization (a) without applied field and (b) with applied field.

1.1.4 Electronic polarization

The electron clouds of every atom shift as the electric voltage is applied to a particular thickness of the sample, which results in net electronic polarization. The shift of the +ve and -ve charges inside the material from their previous position to make a dipole under the application is referred to net electric polarization. Figure 1.5 shows how electronic polarisation works, before and after applying an electric field, valence electrons are contained within covalent bonds. The high dielectric constants of covalent crystals are caused by this kind of polarization. Ge crystals, for instance, have a dielectric constant value of 16.

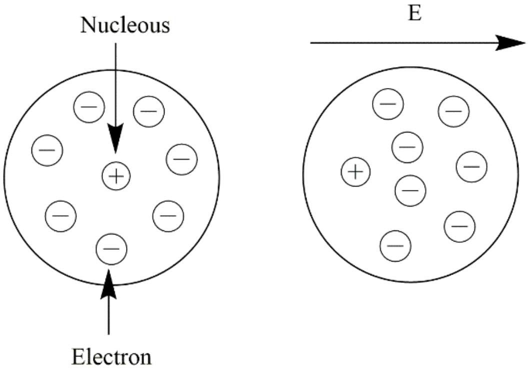

Figure 1.5 Showing the shifting of the charge on the application of the field.

In the presence of various types of polarizations, it can be shown that how the dielectric constant is varying with the time and frequency. Ionic, electrical, and orientational polarization all need a very short period of time (10^{-5} seconds) to polarize and depolarize [13,19,23,24]. Depending on the charge carrier types and dielectric system, interfacial polarization and depolarization take quite a long period. As the frequency is increasing the contribution of the interfacial polarization is decreasing and seems not to present at higher frequencies, this could be due to the reason that at higher frequency of electrical field, the space charge is not able to follow the electrical field. The time taken in the polarizing process by the particular polarization is shown in the Figure 1.6(a). Figure 1.6 (b) and (c) shows the frequency-dependent contribution of several polarization mechanisms to permittivity [13,19,23,24].

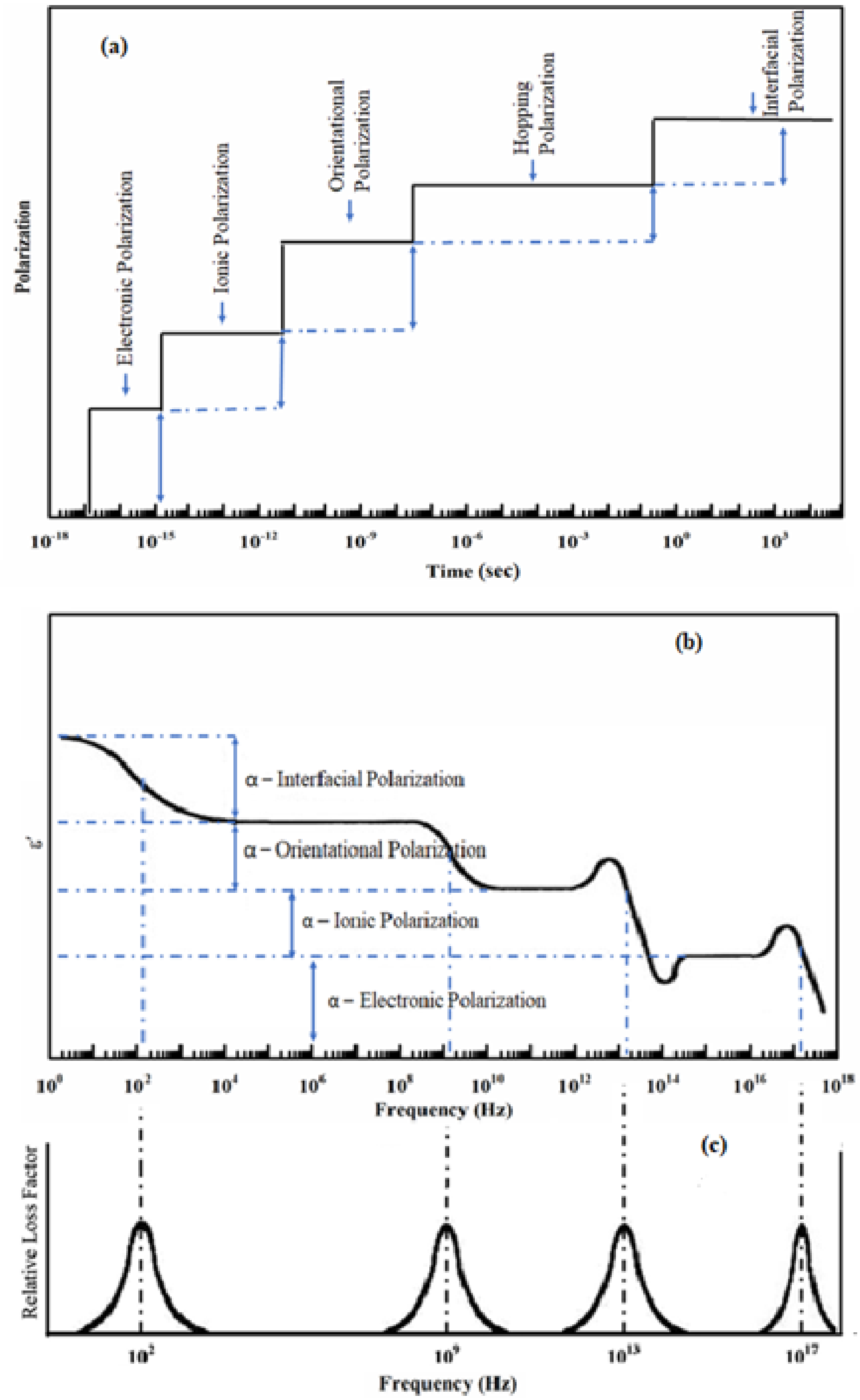

Figure 1.6 Types of polarization varying with time and frequency.

For some special crystal structures, the centres of the positive and negative charge may not coincide even without the application of an external electric field. A spontaneous polarisation is thought to exist in such crystals. Ferroelectric materials are those whose spontaneous polarisation can be reversed by an electric field [25]. The deformed crystal structure or symmetrically extended as the central cation is displaced in one direction is the cause of the spontaneous polarisation [26].

For simplicity we can take example of the Figure 1.7 that is showing the cubic and tetragonal crystal structure in which the cation B is shifted at room temperature which gives rise to the spontaneous polarization [26].

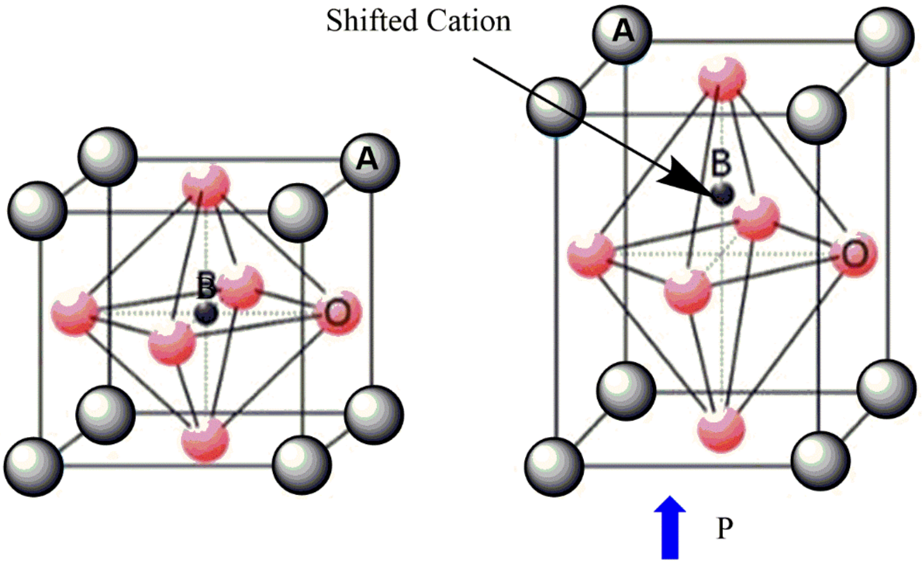

Figure 1.7 Schematic diagram showing the shifting of the cation of the perovskite structure below the curie temperature.

Further, the Figure 1.8 shows the polarization vs electric field response to know the difference between the ferroelectric, paraelectric and linear dielectric materials. Ferroelectric materials have the dipoles in one direction causing spontaneous polarization in material that can be reversed with the application of field as shown in the Figure 1.8. The linear dielectric materials show the linear characteristic with the electric field and polarization. The paraelectric material have fever all dipoles oriented aligned in one direction showing low loss. The ferroelectric have large amount of the dipoles aligned in one direction having high polarization value.

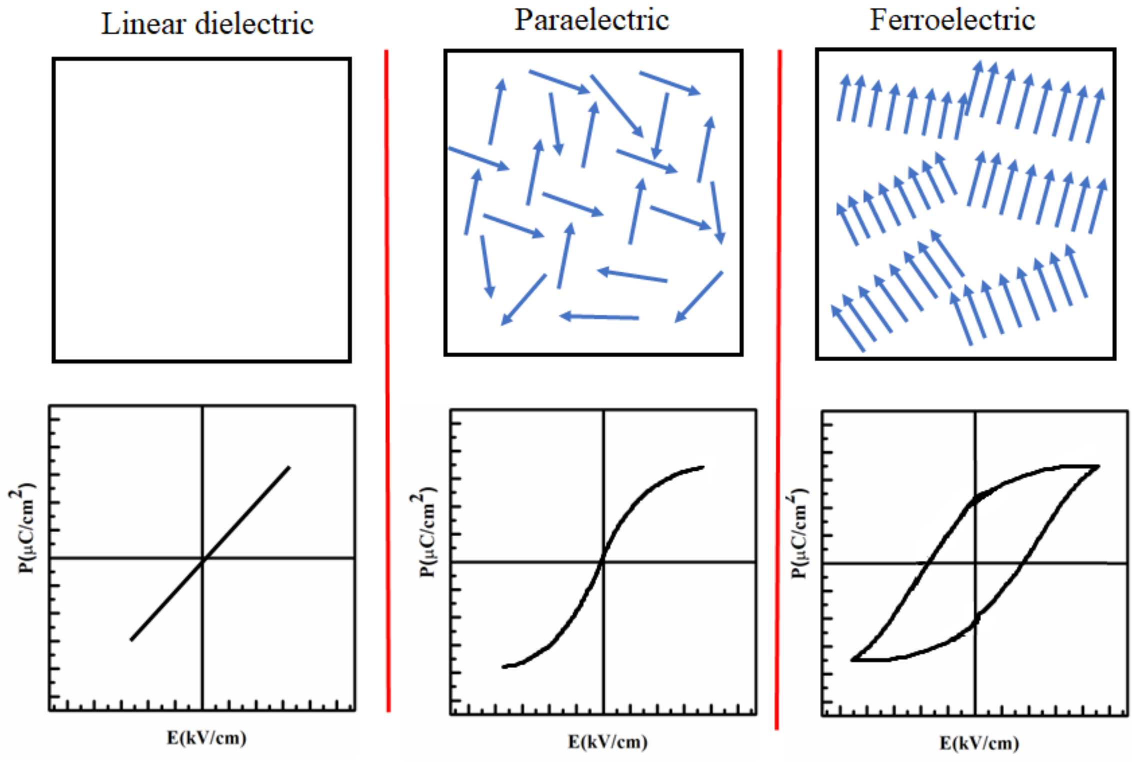

Figure 1.8 Different type of materials under the Polarization and electric field characterization.

1.2 Electrical energy storage

The dielectric materials are classified in the linear and nonlinear according to their characteristics. The linear dielectric materials show linear characteristics between polarization and electric field whereas nonlinear have nonlinear characteristic with hysteresis. A capacitor made up with the linear dielectric material has an energy density that is directly proportional to the square of the electric field applied on the capacitor [25–27]:

$$U_e = \frac{1}{2}\varepsilon_0\varepsilon_r {E_b}^2 \tag{1.9}$$

Where $\varepsilon_r, \varepsilon_0$ are the dielectric constant of material, vacuum dielectric constant (8.85×10^{-12} F/m respectively. The energy density for the nonlinear dielectric materials can't be calculated with the general equation by taking account dielectric constant and electric field simply as there is not obvious linear relation between the polarization and electric field. To calculate the charged energy density of the nonlinear dielectric materials or ferroelectric capacitor, integration the light blue area U_c as shown in figure [25–27], The energy released during the discharging cycle from the per unit volume of material is equal to the discharged energy density of the nonlinear dielectric material. this amount can be calculated by integrating the light blue area U_d in Figure 1.9.

$$U_c = \int E.dP_c \tag{1.10}$$

$$U_d = \int E.dP_d \tag{1.11}$$

$$U_{loss} = \int E.dP_c - \int E.dP_{dc} \tag{1.12}$$

$$\text{Energy efficiency } (\eta\%) = \frac{U_d}{U_d+U_l} \text{ x } 100 \tag{1.13}$$

Where, E is the electric field and P is electric displacement.

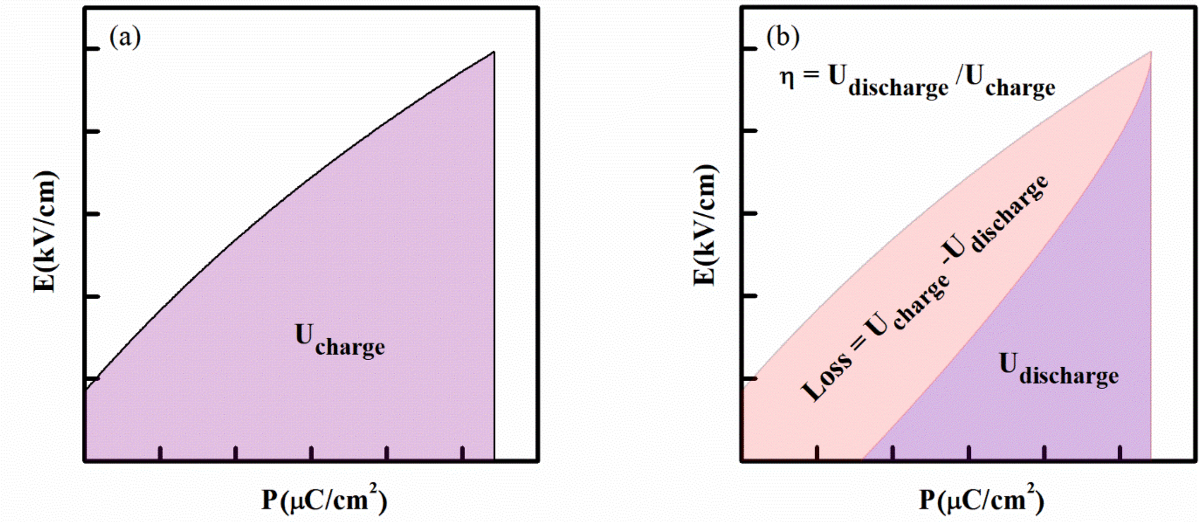

Figure 1.9 Showing the (a) energy stored and (b) energy loss.

High E_b and P are needed for high energy density. Maximum energy density is reached when there is no conduction loss, remnant polarisation at E=0, and coercive electric field at P=0.

1.3 PVDF(Homopolymer) and Its Ferroelectricity

Polyvinylidene fluoride (PVDF) is a semi-crystalline polymer with ferroelectric and piezoelectric properties that is commercially available for usage in a wide range of industrial processes [28]. PVDF has a wide range of applications, energy storage, spanning from electrode binders to biomedical applications, because of its outstanding ferroelectricity, heat stability, good mechanical qualities, and processability[12]. PVDF exists in at least in four unique crystallographic phases: the most common out of which are the α and β varieties as depicted in the Figure 1.10 [12,28]. H and F atoms have the same atomic radius, which allows PVDF for the formation of different crystal forms. As it is cooled from melting, it forms the α-phase, which has a ($TG^{+}TG'$) configuration. With the optimized cooling after melting, the PVDF could have another form, because the H and F atoms reside on opposing sides of the backbone carbon chain of PVDF, which results in a non-zero dipole moment, that is known as electroactive β-polymorph with an all-trans-conformation having spontaneous polarization [2,29,30]. PVDF's electroactive β-phase has been made possible using a variety of methods, including uniaxial or biaxial stretching, high electric field application, thermal annealing, and mechanical rolling. PVDF crystals have a well-documented ferroelectric characteristic [2,29,30]. The introduction of a sinusoidal electric field results in hysteresis, whereas an external electric field reverses polarisation (piezoelectric constant or electric displacement). Due to the presence of net dipoles in their unit crystal cells, the polar crystal forms of PVDF, β-, γ-, and δ- phases display ferroelectric characteristics. A strong electric field makes them exhibit high dielectric constants [6,31]. The α-phase, on the other hand, is nonpolar and hence has low polarization since it does not contribute to polarisation due to non-aligned dipoles. The α-phase may be changed into the β-phase, which has a high ferroelectricity, by applying various processing methods.

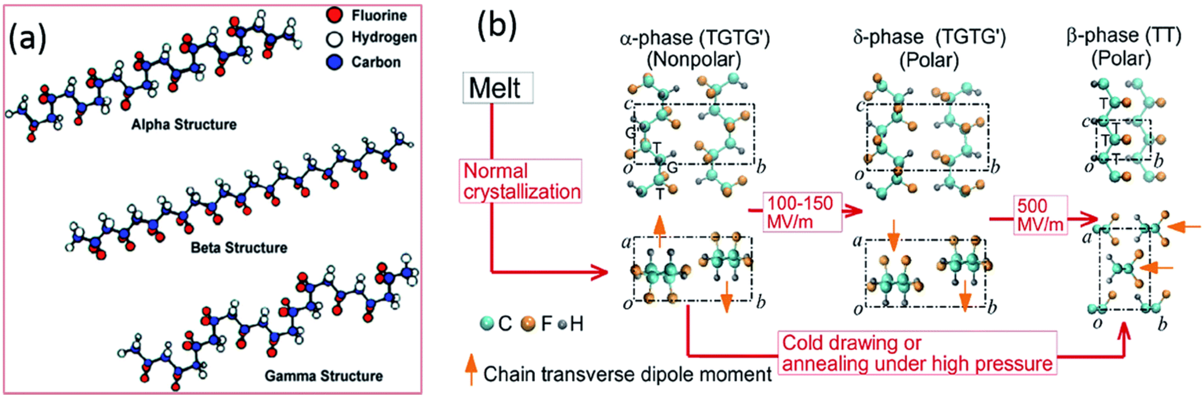

Figure 1.10 (a) PVDF with different phase and (b) Process of the transformation of the phases of the PVDF [6].

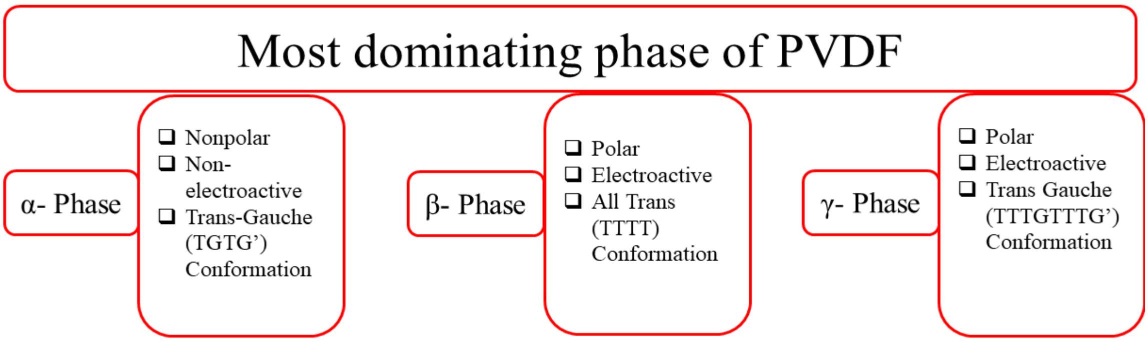

Most dominating phase of PVDF

α- Phase

- ❑ Nonpolar
- ❑ Non-electroactive
- ❑ Trans-Gauche (TGTG’) Conformation

β- Phase

- ❑ Polar
- ❑ Electroactive
- ❑ All Trans (TTTT) Conformation

γ- Phase

- ❑ Polar
- ❑ Electroactive
- ❑ Trans Gauche (TTTGTTTG’) Conformation

Figure 1.11 Dominating phases of PVDF with their characteristics.

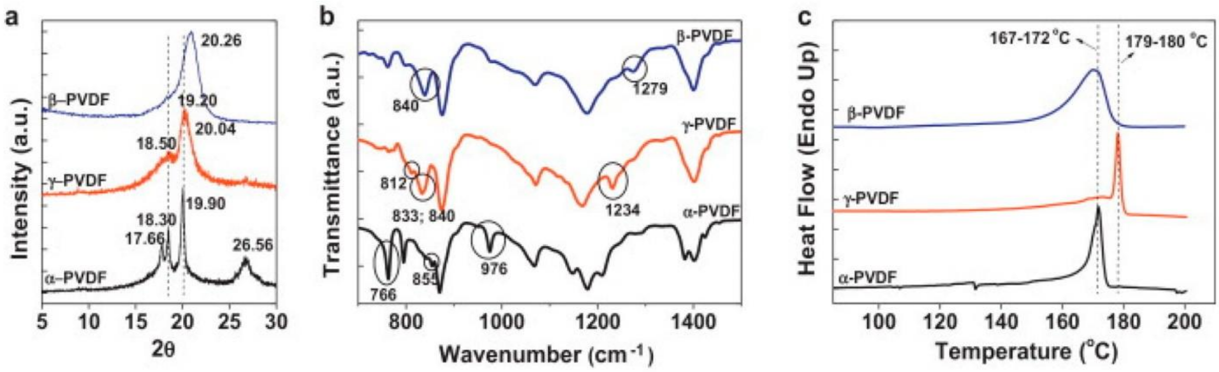

Figure 1.12 (a) XRD, (b)FTIR and (c) DSC plots of the different phases of the PVDF[6,31]

PVDF is ferroelectric polymer as above described and depicted in the Figure 1.11 and 1.12, The ferroelectricity of the PVDF was first discovered by the Naegele and Yoon using an

IR spectroscopy to study molecule dipole ferroelectricity. The transition moment at parallel to and along the CF_2 dipole were having two IR absorptions at 512 and 446 cm^{-1} confirming the ferroelectricity in PVDF [6]. Kepler and Anderesen found that the X-ray diffraction (XRD) analysis of the poled and unpoled samples showed that applied electric field aligned the axes of crystalline region of the PVDF leading to the occurrence of molecular orientation in the 60 degrees increment [32]. Dvey-Aharon and colleagues studied that an increment of 60 degrees, in conjunction with a moderate lattice distortion, was more favourable from an energetic standpoint than an increment of 180 degrees [32]. The Figure 1.12 shows the XRD, FTIR and DSC plots demonstrating the different phases. DSC shows that the thermal stability of the γ-phase is better with the other phases. The DSC is better techniques to know the phase of the prepared samples.

1.4 Percolation threshold and interface phenomena

The critical reinforcement concentration is what determines the electrical percolation threshold. This is the point at which the nanocomposite suddenly transforms from a dielectric nature to partial conducting nature when conductive pathways are generated [33]. These phenomena take place when we are using semiconducting or conducting filler as reinforcement in the PVDF matrix.

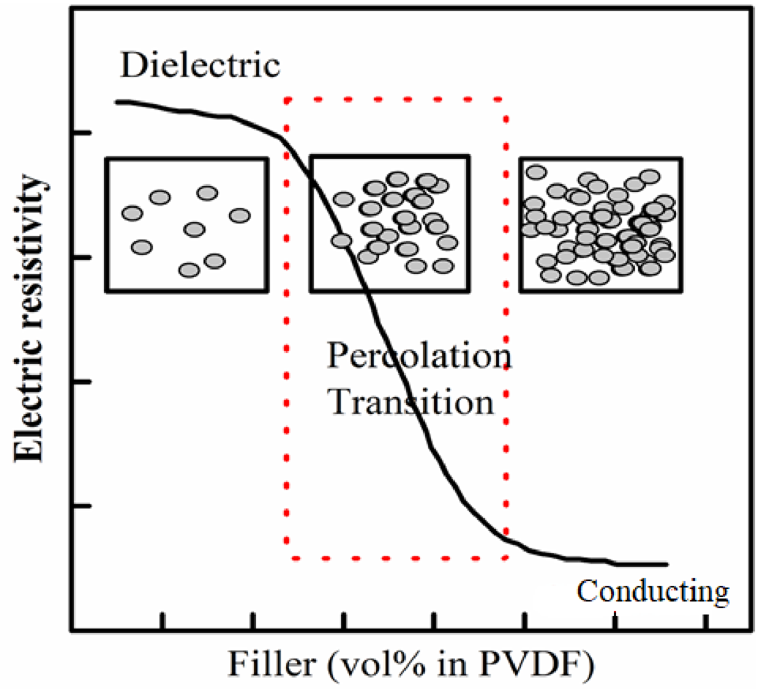

Figure 1.13 Schematic diagram showing the percolation process

The concentration of the filler can be known by reinforcing the filler with varying amount until the conducting nature is not achieved or breakdown strength is lowest with high loss. We can also calculate the critical filler ratio using theoretical methods.

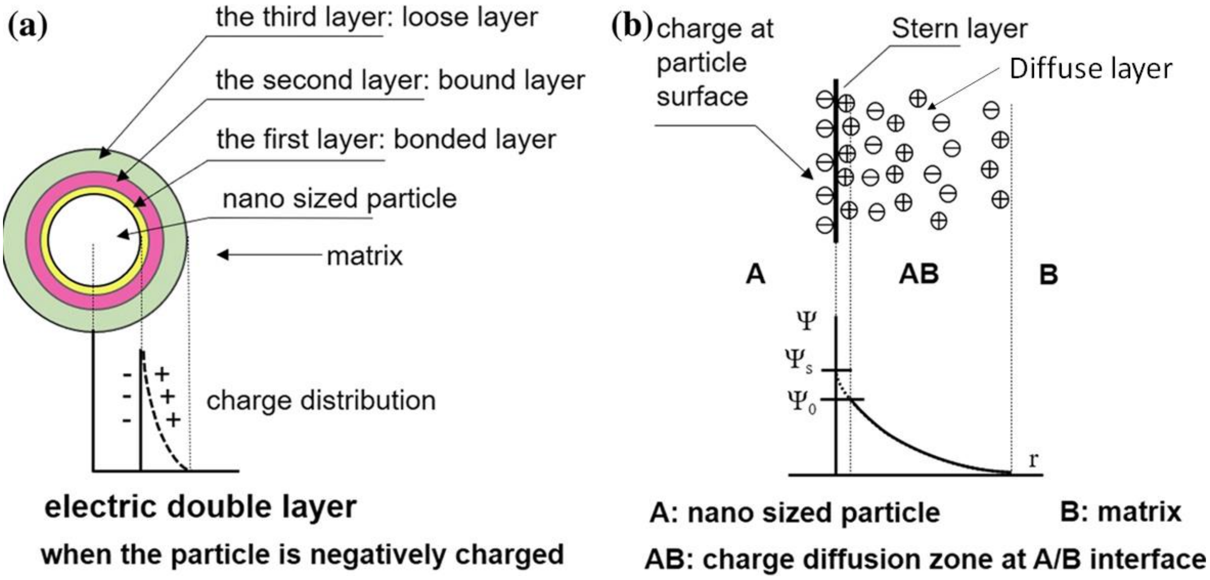

Figure 1.14 Schematic diagram of the interface and dual layers [35].

It is well known that there is interface between the semiconducting filler and polymer matrix. This interface is responsible for the enhancement of the dielectric properties but after a particular amount of the reinforcement interface thickness play important role in the dielectric properties of the nanocomposite films [34].

The previous reports find that the interface may affect the motion and distribution of the space charge that contribute as space polarization enhancement, and it also function as scattering locations that extends the carrier path length resulting in higher breakdown strength[36–38]. Interface can act as traps to stuck the charge affecting the mobility and conductivity, the modification in the electronic state of the interface changes the depth of these trap which further regulate the interfacial polarization and breakdown strength. Space charge (interface) region can alter the polymer molecular structure that initiate from the space charge region to the matrix that leads to affect the dielectric properties[35].

There are various models which are used to describe the polymer matrix and filler interfacial interaction in the nanocomposites. Tanaka model is famous model, it is a multicore model to deal with the interfacial interaction[39]. As the Figure 1.14 shows, It has divided the interface layer into three layers (i) the bonded layer, (ii) the bound layer and (iii) the loose layer. The polymer network and semiconducting filler have the tightly bonded layer based on the polymer network, the interaction holding these chains on static position are hydrogen bonding, electrostatic and Van der waals forces refers to bonded layer with ~1nm thickness [40–43]. This layer is responsible for the prevention of dipole formation causing reduction in the relative permittivity. Second or middle layer is bound layer having strong interaction with bonded layer and surface of filler, the thickness of the bound layer is 2nm to 9nm may vary with interfacial interaction strength. Structures formed by the polymer chains in the bound layer surrounding the filler nanoparticle influence the folding, mobility, and conformation of the chain. The loose layer is the last layer that interact with the bound layer loosely which can alter the conformation of the polymer matrix. Due to the overlapping of the loose layers, which produces an area with combined effects from individual filler particles, the influence of the fillers on the macroscopic characteristics of the composites is amplified at high filler levels. This is the case even though the influence of the fillers is not increased overall. The nanofiller particles and the polymer matrix have different fermi levels so the surface of the nanoparticles has different potential than the polymer matrix. The Gouy chapman diffused layer and stern layer are formed on the surface of the nanofiller particles [39,40]. This is called double layer model given by Lewis to study the polymer nanocomposite interfacial interaction [44].

The surface states of immobile charged impurities, trapped carriers, mobile electrons, and holes in the nanoparticle produce a layer with a positive potential ψ_s when the surface of the nanoparticle is positively charged. The negatively charged Stern layer on the nanoparticle surface includes small molecules, specific absorbed ions, and solvated ions and cannot move freely. The Helmholtz plane (OHP) has ψ_o electrical potential outside this layer [45].

The Gouy–Chapman diffused layer is an extension of the OHP into the polymer matrix; it is developing around the Stern layer by a dispersion of negative and positive ions. This layer may function as a "interaction zone" to influence the nanocomposite's dielectric and electrical characteristics. The electrical potential $\psi(r)$ across the interface area influences the distribution of charges in this layer. The magnitude of $\psi(r)$ varies with the distance (r) from the particle surface and is represented by a combined Poisson–Boltzmann equation [46]; the $\psi(r)$ function is seen below .

$$\nabla^2 \Psi(r) = -e\varepsilon^{-1} \sum\nolimits_{\mathrm{i}} z_i \mathrm{n}_i(\infty) e^{-\mathrm{z_i e}\Psi(r)/kT} \tag{1.13}$$

When the potential is small, the $\psi(r)$ can be reduced to the simple Debye–Hückel [39] form, as shown below.

$$\Psi(r) = \Psi_0 \mathrm{e}^{-\mathrm{kr}};\ K = \left(\frac{2\mathrm{e}^2}{\varepsilon \mathrm{kT}} \sum\nolimits_i \mathrm{z_i^2}\, \mathrm{n_i}(\infty)\right)^{1/2} \tag{1.14}$$

Where, ε = relative permittivity, k = Boltzmann constant, K = Debye–Hückel parameter (m^{-1}), the 1/K is Debye length (L_d). z_i and $n_i(\infty)$ are the ion valency and concentration of ion species i in the bulk polymer matrix, respectively.

The Debye length[47] further can be simplified as:

$$L_d = \sqrt{\frac{\varepsilon_0 \varepsilon_r kT}{e^2\, Nd}} \qquad (1.15)$$

Where, ε_0 , ε_r are the permittivity of the space and material, e =charge of electron, N_d = charge density of the filler, T is temperature in kelvin.

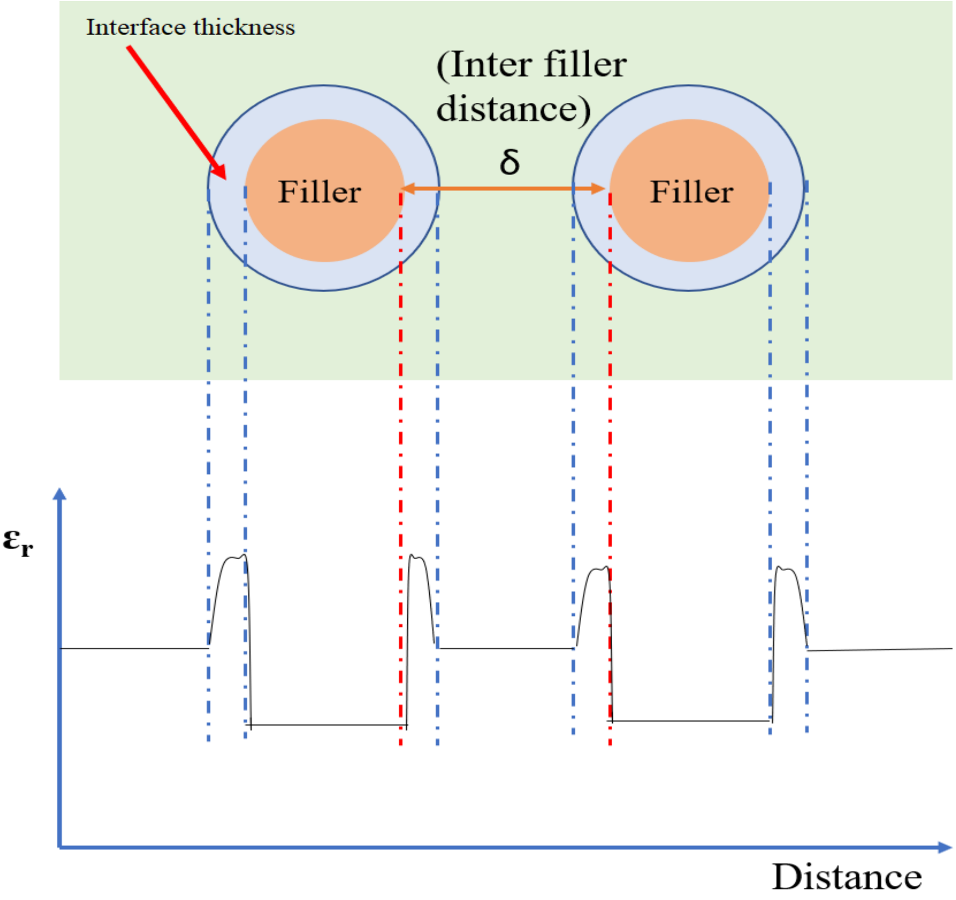

Figure 1.15 Diagram showing the interface and inter-filler distance with dielectric constant variation.

Wu et al[48] developed the formula for the inter filler distance (δ_i) (surface to surface of the nanoparticles) which is as given below:

$$\delta_i = d\left[\left(\frac{\pi}{6\varphi}\right)^{1/3} - 1\right] \tag{1.16}$$

Where, d is nanofiller size (diameter) and φ is filler volume fraction.

The inter filler distance and Debye length could be used to know the critical filler loading in the nanocomposite. If $L_d < \delta_i$ then the interface surrounding the particle will not be interfering to each other. However, $L_d \geq \delta_i$, when the large amount of the filler is reinforced in the nanocomposite then the diffuse layer of each other starts overlapping, this layer has mobile ion which affects the polarization of the nanocomposite. When the electrical field is applied, the ion migration starts which leads to early breakdown of the nanocomposite [35,41,49].

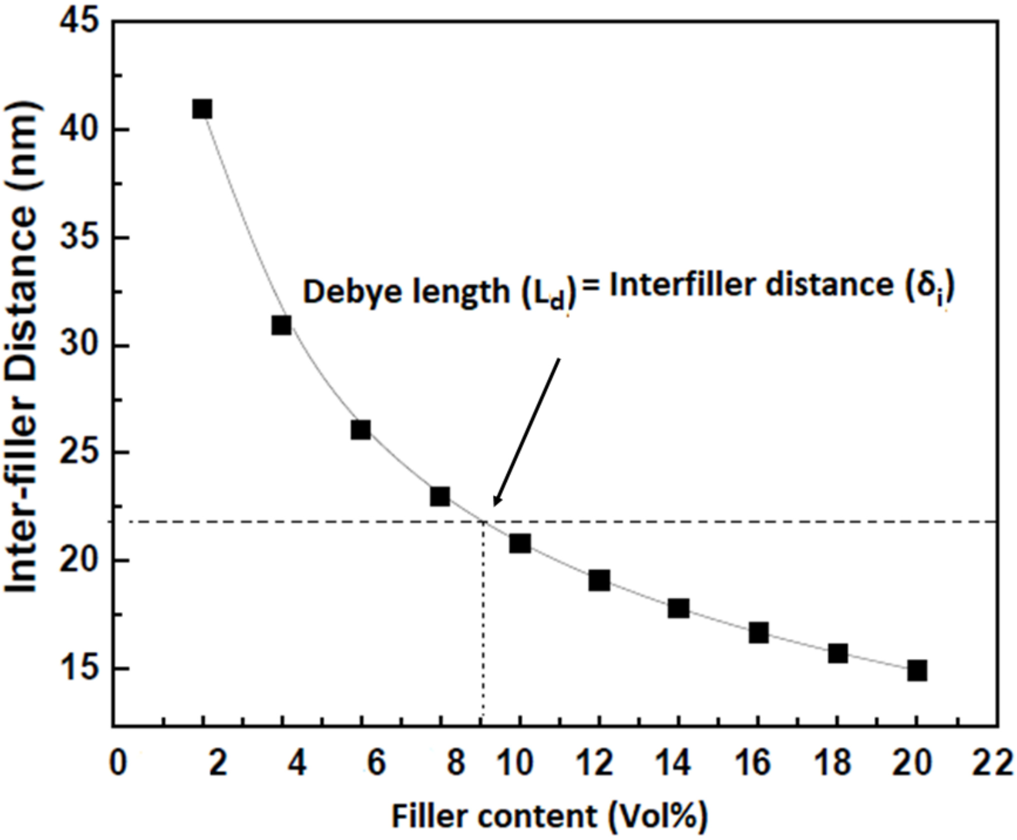

Figure1.16 Showing the tradeoff between filler content in PVDF matric with Debye length and inter-filler distance.

1.5 Breakdown Strength of dielectric materials

The maximum voltage that polymer nanocomposite dielectrics can withstand before deteriorating electrically and chemically is known as breakdown. the dielectric breakdown strength is the maximum applied electric field that a dielectric can sustain[17,50]. There are mechanical, thermal, and electrical processes that can break down polymers. Typically, the creation and spread of electrical trees in the dielectric layer is attributed to the electronic avalanche mechanism as the cause of the dielectric breakdown in polymers. The creation of electrical trees that eventually spread across the top and bottom electrodes and result in breakage is mostly caused by structural flaws in the film. At high temperatures, steady state or impulse thermal processes start the thermal breakdown process. Above a specific critical temperature, an electromechanical mechanism takes control of the breakdown behaviour. Electromechanical breakdown of the dielectric is caused by deformations and softening of polymers brought on by electrostatic forces between the electrodes.

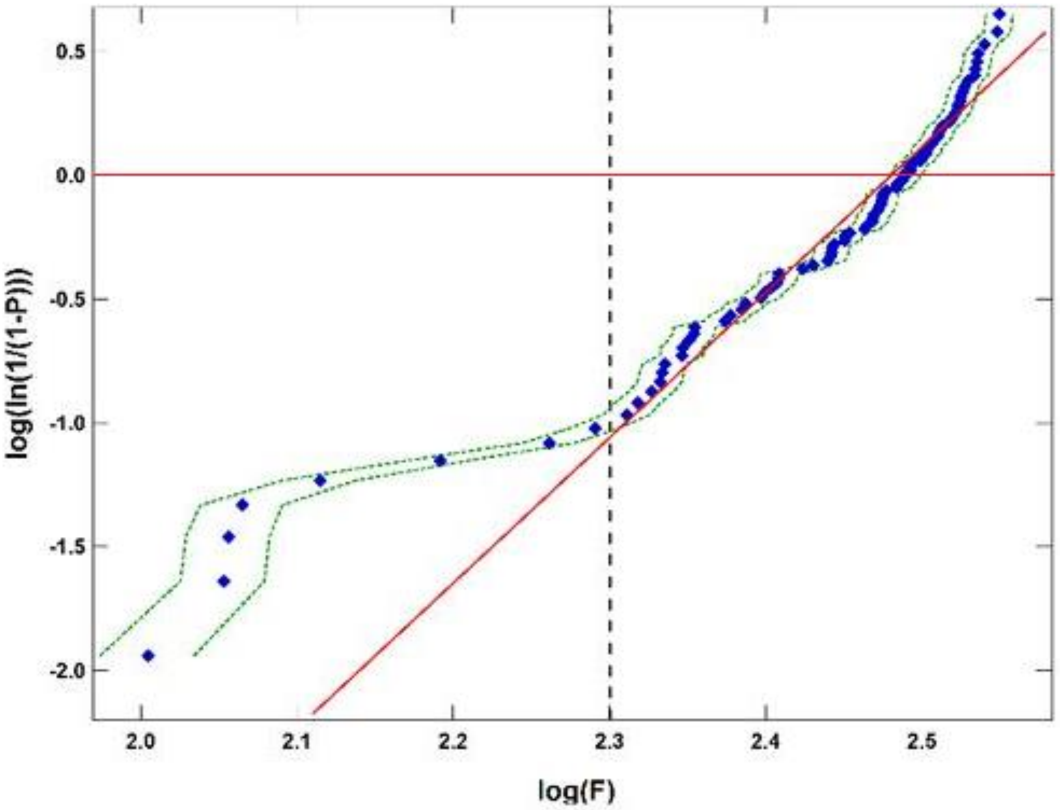

Figure 1.17 plot for the Weibull distribution.

The breakdown strength estimation is done with the help of the of the Weibull distribution function. The breakdown strength analysis is done with the help of the Weibull cumulative probability function given below equation (1.17) [51].

$$P(E) = 1 - exp\left[-\left(\frac{E}{E_b}\right)^{\beta}\right] \tag{1.17}$$

where *P(E)* is the cumulative prospect of electrical breakdown, E is the actual breakdown field, E_b is the breakdown field when the cumulative prospect is 63.2%, and β is the shape parameter obtained by linear fitting, higher β represents the better results in this analysis. we draw a plot between two parameters Xi, Yi given in the equation (5), (6) below and the plot is shown in Figure 1.17 (a).

$$\mathrm{X_i} = \ln(\mathrm{E_i}) \tag{1.18}$$

$$\mathrm{Y_i} = \ln\left[-\ln\left(1 - \frac{\mathrm{i}}{\mathrm{n+1}}\right)\right] \tag{1.19}$$

Where, i is the consecutive number of samples in n numbers of samples, E_i is the experimentally measured value of PVDF and its nanocomposites. β is the shape parameter, the slope of the linearly fitted line. The shape parameter should be higher for a better result, and here we have got a better shape parameter for all samples.

The energy stored in a capacitor is expressed as [2,52]:

$$U = \frac{1}{2}CV_b^2 = \frac{1}{2}\varepsilon_0\varepsilon_r AdE_b^2 \tag{1.20}$$

Where V_b, E_b is defined as the breakdown voltage and breakdown strength respectively. Enhancing the dielectric constant and breakdown strength will enhance the energy density as according to the equation for the linear dielectric materials but for non-linear dielectric materials, enhancing the maximum polarization, reducing the remanent polarization, high breakdown strength, and reducing energy loss with enhanced dielectric constant would improve the energy density of the material.

1.6 Enhancing the dielectric properties and energy density of PVDF

More than a decade ago, it has been shown that the dielectric PVDF polymers might be converted to ferroelectrics by reducing the remnant polarisation and crystal size. Various techniques and synthesis methods have been used by the researchers out of which some major techniques are described below.

1.6.1 Modifying the defects

PVDF have defects when it is processed as films for the application purpose so these defects can be modified to achieve desirable properties [6,53]. Defect modification by irradiation turns ferroelectric polymers to relaxor by lowering the remanent polarisation of PVDF-based polymers using the proton irradiation [6,53]. Chemical alteration is another way to make relaxor ferroelectric polymers. The addition of the TrFE to PVDF in optimized amount resulted in enhancement of dielectric constant and polarization, at PVDF/PVDT-TrFE (60/40), the dielectric constant was increased to ~23 and polarization to $0.125 \mu C/cm^2$ [54]. The addition of chlorofluoroethylene (CFE) like bulky and functional side group to the main carbon chain of the PVDF and P(VDF-TrFE), the dielectric properties can be achieved for high energy density-based capacitors. Chemical defect modification has been used to synthesize the P(VDF-CTFE) and P(VDF-HFP) copolymers. Despite having a dielectric constant lower than 12, these copolymers can achieve high energy densities (>25 J/cm^3) at 600 kV/cm [54]. Defect modification methods need sophisticated irradiation or chemical synthesis (co- or terpolymerization) with precisely regulated reaction conditions and polymer composition, raising material costs and limiting commercial applicability [53-54].

1.6.2 Blending and grafting the polymers

A polymer blend or mixture creates a new material with varied physical properties by combining at least two polymers. This approach improves nonlinear dielectric polymers' dielectric properties [6] . However, Miscibility of polymers affects the homogeneity of blend polymer. Polymer blends have large maximum polarization and minimal remnant polarization. Whereas, the grafting of the polymers is done to modify their structural and electrical properties. The other properties like melting point, hydrophilicity, hydrophobicity, adhesion and crystallinity have also been modified with the grafting copolymerization [55]. Graft copolymers are made up of the homopolymer or copolymers attached to the side of the polymer having different main chain.[56–58]

Blending P(VDF-TrFE) and P(VDF-CTFE) affected the polarization of resulting blend product. Previous studies show that PMMA is miscible with P(VDF-HFP) and P(VDF-TrFE-CFE). Adding ferroelectric polymers to PMMA lowered crystallinity and increased mechanical modulus[58]. Blending ferroelectric polymers with PMMA reduces polymer crystal size, allowing dipoles to flip and reducing remnant polarisation and energy loss. Dielectric characteristics of P(VDF-TrFE-CFE) terpolymer and P(VDF-CTFE) copolymer blends were studied by the Shezad et al [59]. The enhancement in the dielectric constant and energy density were significant. Blending of low amount of copolymer with terpolymer improved polarization response and electric breakdown strength caused by the interfacial interaction or interfacial polarization and elastic modulus improvement. It has well known after lot of research recently that blending is a straightforward and cost-effective strategy for enhancing the dielectric characteristics and modifying polymer properties for energy storage applications[56].

In a 20-year-old study, polystyrene (PS) was used to modify the PVDF utilising electron beam (EB) induced free radical graft copolymerization (EIGC) [60]. The enhancement in the dielectric properties of the grafted PVDF was studied and enhancement in the dielectric constant was very promising with a value of 90 the breakdown strength (400 kV/cm) was higher than PVDF. Similarly, HEMA-was further used to graft the PVDF copolymers using free radical graft copolymerization which resulted in enhancement in the value of the dielectric constant was higher than 47 and the dielectric loss was 0.002 [61]. Overall findings of the research are that graft copolymerization can improve dielectric and storage properties of the nonlinear dielectric polymers.

1.6.3 Using different filler to synthesize the PVDF based Nanocomposite

This section describes the synthesis process, physical, structural and dielectric properties of the PVDF based nanocomposite with the various nanofillers. The effect of the characteristics of the Nanofiller on the nanocomposite films. The nonconducting and conducting type of fillers can be used to enhance the electrical properties, further these fillers can be divided into the shapes of the nanostructures.

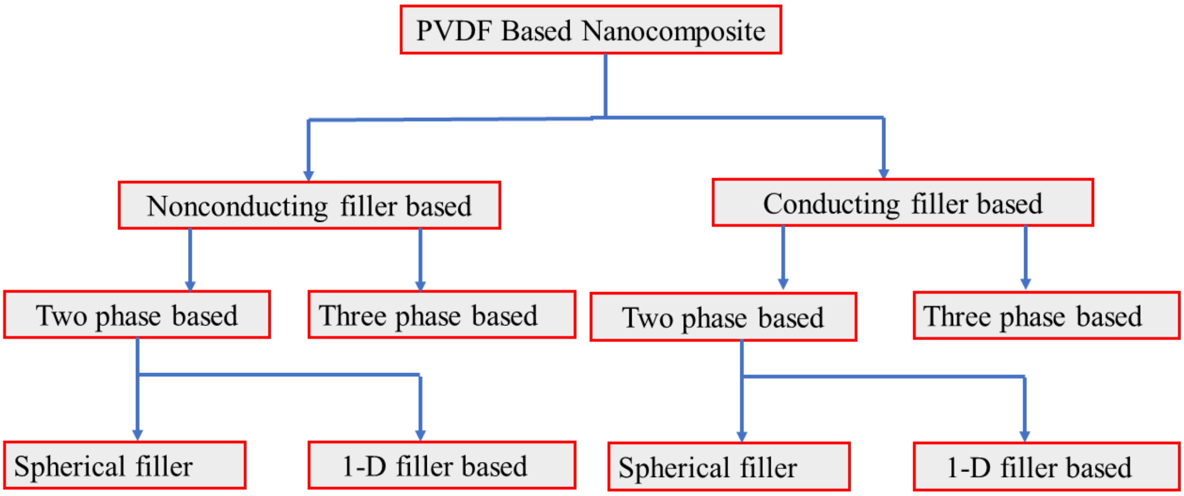

Figure 1.18 Classification of the PVDF based Nanocomposites [6].

1.6.3.1 Nanocomposite based on Nonconducting fillers

In non-conducting fillers, this section discusses two-phase polymer nanocomposites using nonconducting PVDF fillers. Ceramic nano-fillers like $BaTiO_3$, $SrTiO_3$ etc., are popular nonconducting fillers [2,12]. The dielectric properties of a various nanocomposites based on $BaTiO_3$ are reviewed here. Mao et al.[62] explored dielectric characteristics of $BaTiO_3$/PVDF nanocomposites depending on the diameter of the filler particles. At 60 vol% of filler loading, the dielectric constant increased from 52 to 95 with an increment in diameter of $BaTiO_3$ from 50 to 100 nm, then fell to 70 at 500 nm at 1 kHz. The value of dielectric constant increased due to the structural transformation of $BaTiO_3$ from cubic to tetragonal with diameter variation. Due to non-symmetry of tetragonal structure, $BaTiO_3$ in tetragonal structure has better polarization, thus helps in increment in the dielectric properties of PVDF nanocomposite at room temperature [62]. The Figure 1.19 shows the enhancement due to the $BaTiO_3$ reinforcement in PDVF.

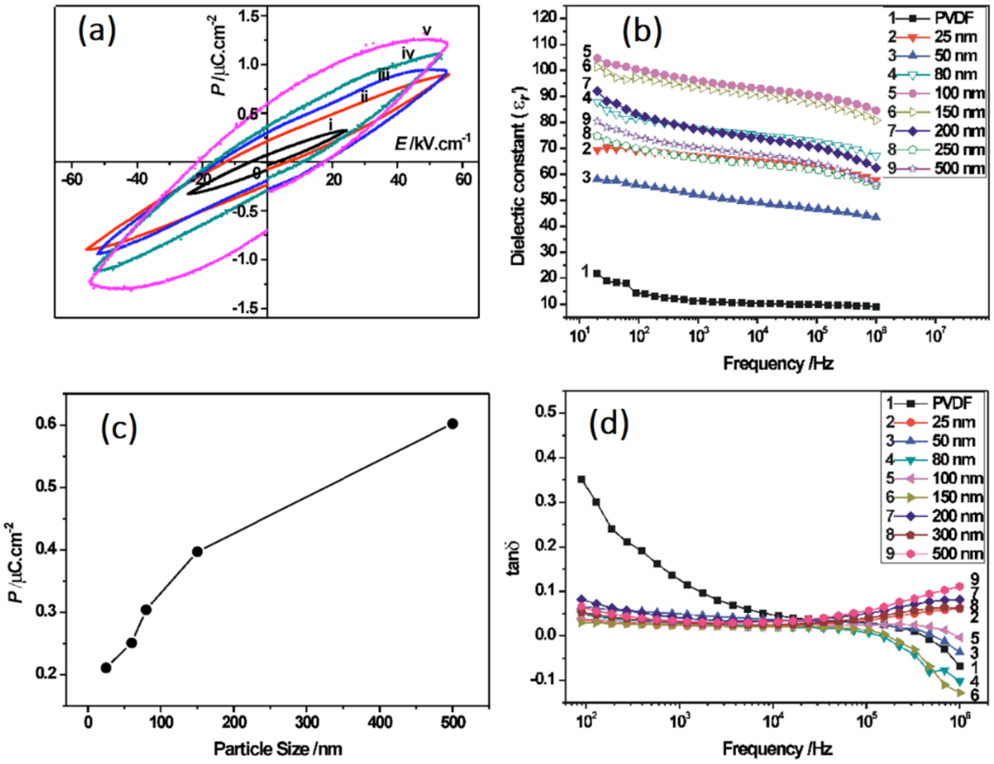

Figure 1.19 (a) PE loop, (b) Dielectric constant, (c) Polarization variation, (d) Loss of the $BaTiO_3$/PVDF with the size of the filler particles [62].

Modelling is needed to understand the mechanism behind the reduced dielectric constants for diameters exceeding 100 nm. PVDF nanocomposite have 0.1 loss tangent at low-frequency recorded at all diameters variation of the filler. The value of tanδ was 0.05 at 1 kHz at 60% vol loading of filler. Further, PVDF's partial conducting nature and interface effects led to a higher value 0.13 of tanδ at frequency of 1 kHz. The doping and nanoparticle surface modification can help in reducing the dielectric loss of the nanocomposites.

$BaTiO_3$ nanoparticles having diameter of 85-100 nm were treated with H_2O_2 to study its dielectric characteristics by the Zhau et al. [63]. H_2O_2-modified $BaTiO_3$ reinforced PVDF nanocomposite have improved morphology due to the hydrogen bonding with fluorine. Nanocomposite with H_2O_2-$BaTiO_3$ have better and steady dielectric constant varying with frequency and temperature compared to crude $BaTiO_3$ as the side groups have less mobility and interface interaction of the polymer. The values of dielectric constant and tanδ at 30vol% loading of $BaTiO_3$ in PVDF was recorded 25 and 0.02 respectively at 20 °C, enhanced to 32 and 0.2 respectively at 150 °C. Whereas, for the same amount loading of modified $BaTiO_3$ in PVDF matrix, the value of the dielectric constant of 28 at 20 °C and 50 at 150 °C and a tanδ of 0.03 and 0.5. The tanδ of modified filler reinforced PVDF nanocomposites was always less than the 0.14 in all frequencies range of 100 Hz to 1 MHz [63]. The surface modification of the filler shows the low dielectric loss and stability at higher temperature as well which is desirable.

Wang et al.[64] incorporated the $SrTiO_3$ nanoparticles (NPs) in PVDF matrix. To establish good bonding, interaction and compatibility with PVDF Matrix, the $SrTiO_3$ NPs were surface modified with the help of polyvinylpyrrolidone (PVP). The Figure 1.20 demonstrate the impact of the surface modification on the dielectric and storage properties. Surface modification enhanced the polar phase. PVDF based Nanocomposite films with 5 vol% surface modified $SrTiO_3$ NPs show enhancement in energy density to 5.1 J/cm^3, which is 1.82 times of the pure PVDF. This enhancement can be attributed to the fact that the PVDF/PVP@$SrTiO_3$ contain surface modifications of the filler that made better nanocomposite with the low dielectric loss. In addition, the PVDF nanocomposites have high value of energy efficiency of 80.7% at an applied electric field below than the 1000 kV/cm and maintained at higher than 64.6% with field of 2700 kV/cm. This is the case regardless of the magnitude of the electric field. According to the findings, the nanocomposites films that make use of surface-modified paraelectric fillers have high energy storage densities and high efficiencies.

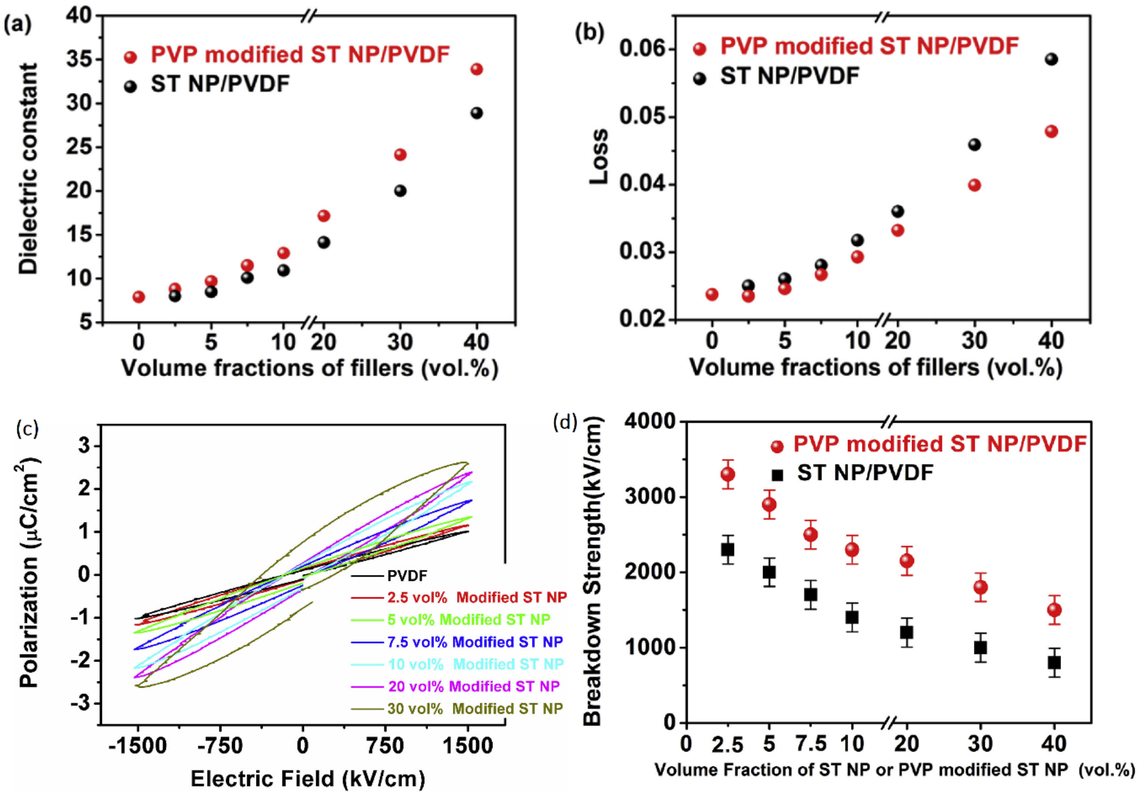

Figure 1.20 (a) Dielectric constant, (b) Loss, (c) PE loop, (d) Breakdown, of the PVP modified ST NP/PVDF and ST NP/PVDF with the size of the filler particles [64].

The $BaZr_{0.2}Ti_{0.8}O_3$ (BZT) nanofibers were synthesized and further coated with polydopamine (PDA by the Want et al.) [65]. The PDA coated BZT nanofibers were used as the filler in PVDF matrix. The PDA introduces and improve the compatibility between the BZT nanofibers and matrix. The enhanced energy density was up to 13.0 J/cm^3 with 5 vol% BZT filler at 5219 kV/cm, quite larger than that of PVDF (~ 6.6 J/cm^3 at field of ~ 4447 kV/ cm). Wang et al. also used phase field simulation to show the electrical field distribution to depict the improvement in the breakdown strength that can be attributed to the PDA coating of the BZT nanofibers. The method is realistic path toward obtaining good energy density of the nanocomposites under modest filler loading, promising application prospects to the next generation of electrical micro capacitors.

Lou et al.[66] synthesized the heat conductivity core SiC and $BaTiO_3$ as shell to load as filler in the P(VDF-HFP) based nanocomposite, The Figure 1.21 demonstrates the enhancement in the dielectric and storage properties. The 7.5wt% filler loading in the PVDF matrix enhanced the energy density and breakdown strength at high temperature. The pure PVDF has energy density of 0.36 J/cm^3 at 700kV/cm whereas the nanocomposite has 2.05 J/cm^3 at 1700kV/cm at 120℃. The SiC have high heat conductivity which helped in maintaining the storage properties at the higher temperature. At higher temperature, the gain in thermal breakdown strength along with the electromechanical breakdown strength was attributed to the improvement in thermal performance and Young's modulus of materials.

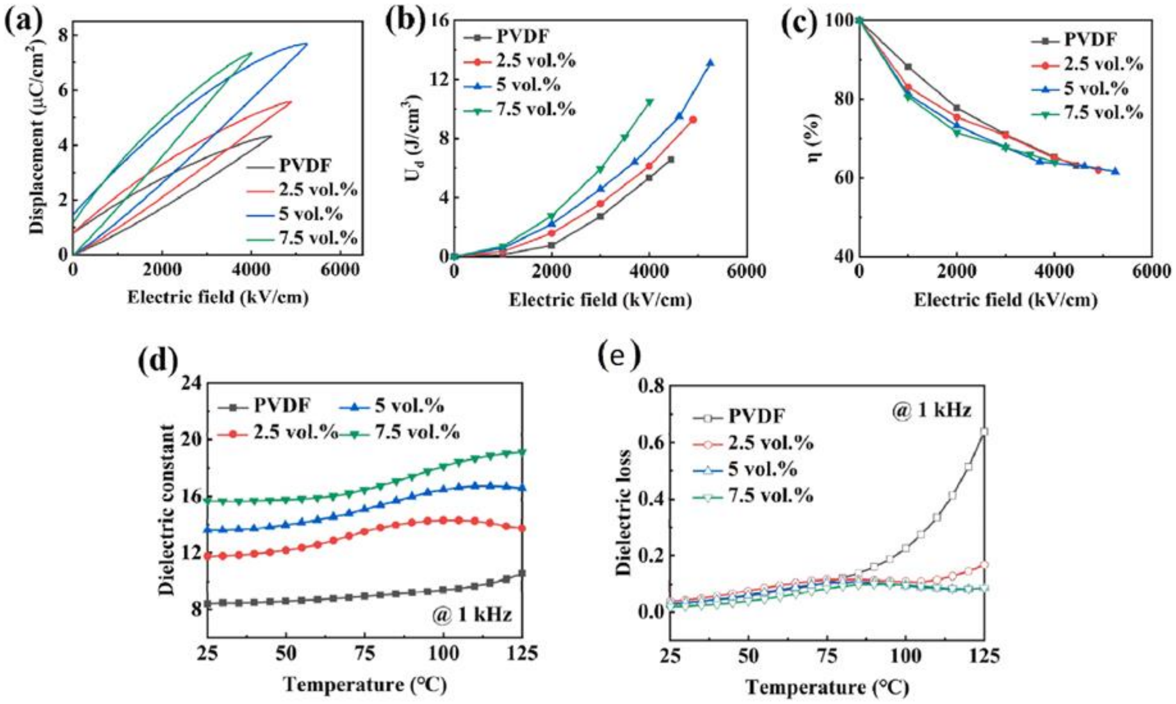

Figure 1.21 (a) PE loop, (b) Dielectric constant, (c) Polarization variation, (d) Loss of the $BaTiO_3$/PVDF with the size of the filler particles [66].

Ye et al.[67] functionalized $BaTiO_3$ with 1-tetradecylphosphonic acid (TDPA). TDPA, a 14-carbon chain molecule, created less steric hindrance and offered greater surface coverage than rigid benzene-ring phosphonic acids. The 40vol% of the filler reinforcement in the PVDF enhanced the dielectric constant 48 and 33.8 at the 1kHz and 1MHz respectively, for the same amount of loading the tanδ increased to 0.15. Even at 40% vol, the nanocomposites remained flexible. TDPA surface modification enhance the dielectric constant of nanocomposites and reduce the dielectric loss, and flexibility at larger loadings. Metal nanoparticles are sometimes used to modify the insulating ceramic nanofillers. Xie et al. [67] achieved the desired dielectric and storage properties by developing the core satellite nano assemblies using $BaTiO_3$ and Ag nanoparticles. The achieved dielectric constant at the loading of 20vol% $BaTiO_3$ with 1%, 0% of Ag was 16 and 20 respectively, while the loss was 0.02 for both, the addition of the BaTiO3 with Ag has lower dielectric constant because of the greater activation energy, the charge build up in different of the PVDF increases the energy requirement to move the space charge Coulomb blockade effect is the reason for the low dielectric loss in the nanocomposite. The quantum confinement effect limits the movement of the charge in the Ag nanoparticles [67]. The energy density calculated at the field of 600 and 1000kV/cm respectively for the PVDF based nanocomposite loaded with 20 vol % Ag@$BaTiO_3$ (0.335 and 0.83 J/cm^3 respectively) have higher values in comparison of the 20vol% of $BaTiO_3$ loaded PVDF (0.242 J/cm^3 at 600kV/cm) with breakdown at 1000kV/cm. Luo et al. deposited Ag nanoparticles (5-20 nm) to modify the surface of the $BaTiO_3$ nanoparticles. At 56.8% loading having 8.2% Ag on the surface of 48.6% of $BaTiO_3$, the achieved value of the dielectric constant was 160, 16 times that of pure PVDF. The dielectric constant of PVDF nanocomposite reinforced with 8.2 vol% Ag and 48.6 vol% $BaTiO_3$ is 160 whereas 10 for the pure PVDF, this increment in the value of the dielectric constant is due to interfacial charge and better distribution of the filler particles in PVDF matrix. The value of the dielectric loss was <0.1 at 100 kHz and <0.26 at at 100 Hz to 10 MHz respectively. Dielectric constant was moderate at the percolation threshold due to strong bonding interaction between $BaTiO_3$ and Ag nanoparticles. PVDF has low conductivity of <10^5 S/m up to 1 kHz.

Xu et al. [68] reported the enhancement the storage properties of PVDF nanocomposite as follow: TiO_2@$SrTiO_3$@polydamine nanowires (TiO_2@$SrTiO_3$@PDA NWs) was incorporated in the PVDF. The filler loading at 5 wt% of TiO_2@$SrTiO_3$@PDA NWs in PVDF has enhanced the highest discharge energy density to 10.34 J/cm^3 at 198 kV/cm as compare to the pristine PVDF and efficiency of 69% at the same field. The enhancement can be attributed to the interfacial polarization and large aspect ratio which helped in more interface. The Figure 1.22 shows the increment in the properties. The Figure 1.22 (a) shows the decrement in the breakdown strength as the filler loading is increased.

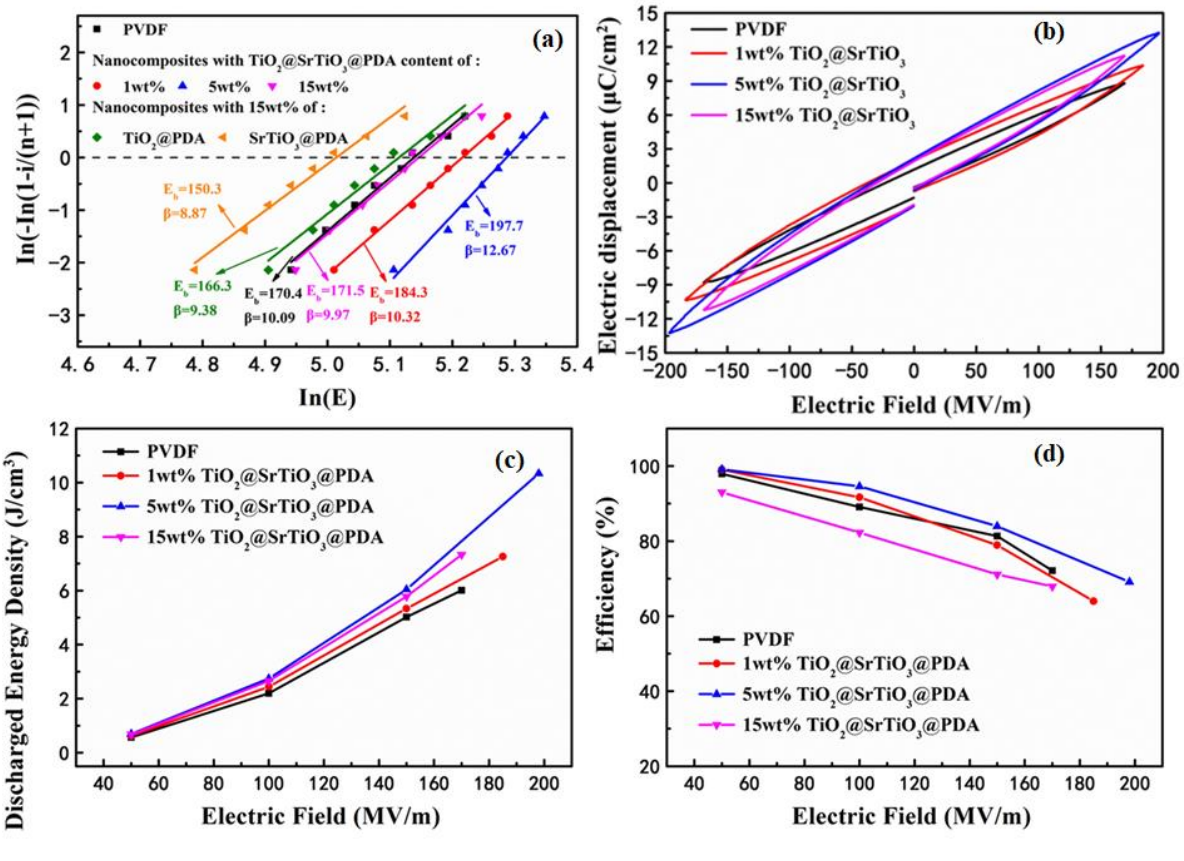

Figure 1.22 (a) Breakdown Strength, (b) PE Loop, (c) Discharged Energy density, (d) discharged energy density of the TiO_3@Sr TiO_3@PDA/PVDF [68].

Li et al. [69] modified the surface of the $Ba_{0.6}Sr_{0.4}TiO_3$ nanoparticles by coating the with Ag and APS. PVDF nanocomposite with $Ba_{0.6}Sr_{0.4}TiO_3$ coated with the Ag nanoparticles have dielectric constant increased from 20 to 125 (at 1 kHz) with the loading increased from 15 to

55 vol% up to the percolation threshold limit. Nanocapacitors formed inside the matrix and the space-charge polarisation boosted performance. At 60% loading, the dielectric constant dropped to 110. As the percolation threshold was reached, the dielectric loss (tanδ) was reached to 0.1 from 0.05 at 1 kHz. Current leakages were incorporated along with the increment in the polarization. As the filler loading rose from 40 vol% to 55 vol%, AC conductivity or leakage current increased from 4.07 x 10^{10} to 1.52 x 10^{9} S/m and then fell to 5.263 x 10^{10} S/m at 60%vol. Conductivity increased with electron transfer and decreased with electron trapping in pores, restricting electron mobility.

Luo et al. [70] used the PDOPA to modify the surface of $Ba_{0.95}Ca_{0.05}Zr_{0.15}Ti_{0.85}O_3$ powders with the diameter of 200-300 nm by coating on the surface to reinforce in the PVDF nano-composites with the help of solution cast method, $Ba_{0.95}Ca_{0.05}Zr_{0.15}Ti_{0.85}O_3$ improves crystallinity of the polymer matrix. PDOPA improved filler compatibility to make better nanocomposite with the polymer matrix, giving the composite up to 52 vol% loading flexibility. At 61% vol filler loading, dielectric constant of the PVDF nanocomposites was 100 at and tanδ was 0.05 at1 kHz. The theoretical models like Jayasundere Smith, Rother Lichtenecker, and Maxwell Wagner, fit well up to 20 vol% loading but above 30 vol % loading in the PVDF, only the modified Rother Lichtenecker model was accounted for shape-dependent factors. As the filler vol% increases, more composite interfaces are created, which must be considered. At 61 vol% percent loading, the breakdown strength was lowest with the value of 679 kV/cm and the energy density was 2.0 J/cm^3. $Ba_{0.95}Ca_{0.05}Zr_{0.15}Ti_{0.85}O_3$ nanoparticles added flexibility and increased electrical characteristics to PVDF nanocomposites. In situ nanocomposites can have a higher dielectric constant without filler surface change.

Wang et al. [71] used the $BaTiO_3$@TiO_2@SiO_2 (BT@TO@SO) to enhance the storage properties of the PVDF based nanocomposite. The core-double shell structured ceramic filler BT@TO@SO have multilayer interface to enhance the interfacial polarization. The dielectric constant value of the $BaTiO_3$, TiO_2 and SiO_2 is very much different from each other, thus this dielectric mismatch reduces the electric field concentration. So, the insulating material which helped in limiting the migration of the electrons and reduce the leaking current in the PVDF based nanocomposite. The low amount the filler provides the good enhancement in the energy density to 19.7 J/cm^3 and moderate efficiency of 57.6%. at 620 MV/m. Energy density was good but the efficiency at higher field was found to be lower.

Yi et. al.[72] evaluated the dielectric properties and energy storage properties of sandwich-structured $Na_{0.5}Bi_{0.5}TiO_3$ Nanofibers/PVDF nanocomposites, The results shown in the Figure1.23 evidenced the enhancement. NBT-NFs (nanofibers)/PVDF has a higher dielectric polarisation strength than NBT-NPs (nanoparticles)/PVDF, hence its dielectric constant is higher. Sandwich-structured helped in achieving the large energy density of 11.7 J/cm^3 at a applied electric field of 3500 kV/cm with only 1% NBT-NFs in the outer layers. Electric modulus and film crystallinity prove NBT-NF-filled composites have higher polarisation. The study also indicated that composites had high stability and bending cycle stability. This is due to the better interfacial interaction with the nanofibers in comparison to the nanoparticles.

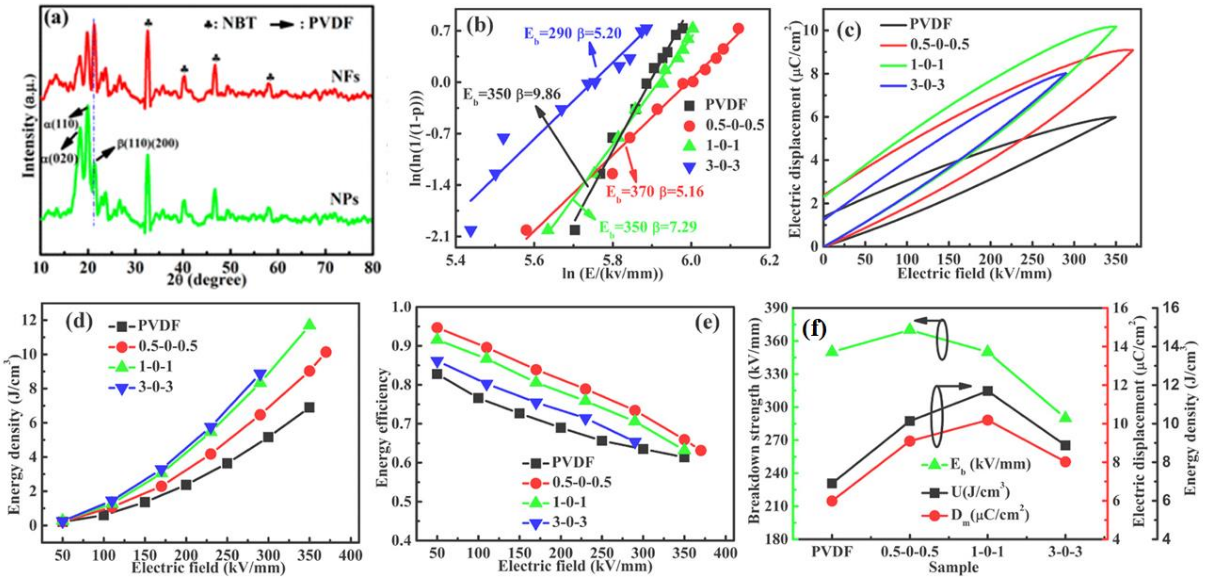

Figure 1.23 (a) XRD of the NBT-NFs and PVDF, (b)Weibull analysis, (c) PE Loop, (d) Discharged Energy density, (e) discharged energy density (f) Breakdown strength variation of the NBT-NF/PVDF [64].

Shaohui et al.[7] employed $Ba_{0.6}Sr_{0.4}TiO_3$, H_2O_2-modified nanofibers. Surface-modification/passivation of the $Ba_{0.6}Sr_{0.4}TiO_3$ nanofibers had a lower dielectric loss than untreated nanofibers due to fewer air spaces. 10 vol% polymer nanocomposites had a dielectric constant of 25. The dielectric loss was lower at a value of 0.01. The nanocomposites have high dielectric constant that can be understand with the help of imaginary electric modulus (M″). With the addition of fillers, peaks shifted and broadened due to charge build-up at the filler-matrix interface, which became more evident with increased loading. The nanocomposite prepared from the filler having surface modified shows very good dielectric breakdown strength of 3980 kV/cm at 2.5 vol% and 2600 kV/cm at 10 vol%. The breakdown strength was higher at lower loading was due to the better interaction because of the surface modification the filler and large aspect ratio of plane-oriented fillers, thus effective electric field was lowered in out-of-plane direction. Higher breakdown strength results in 6.4 J/cm^3 energy density at comparable lower loading.

1.6.3.2 Nanocomposite based on conducting/semiconducting fillers

The conducting fillers are being used extensively to achieve the desired dielectric properties with low amount reinforcement in PVDF. There are various conducting/semiconducting fillers like Ag, Cu, graphene, Si etc.

Samal et al.[73] hydroxylated the $BiFeO_3$ to reinforce it in PVDF matrix. Hydroxylation with H_2O_2 increased the compatibility of bonding with ferrite as it has done with $BaTiO_3$ discussed already in previous section. The Figure 1.24 is showing the increment in the, electroactive phase, storage and dielectric properties. The surface hydroxylation improved the interfacial interaction between the reinforced filler and polymer matric as -OH group is present which introduce the strong hydrogen boing. The interaction of -CF_2 with -OH of the hydroxylated $BiFeO_3$ helped in increment in the polar phase of the PVDF which increased to 91% for a loading hydroxylated $BiFeO_3$ (7 wt%) in PVDF matrix. This interfacial interaction increased the space charge polarization which enhanced the dielectric and ferroelectric properties of the nanocomposite film.

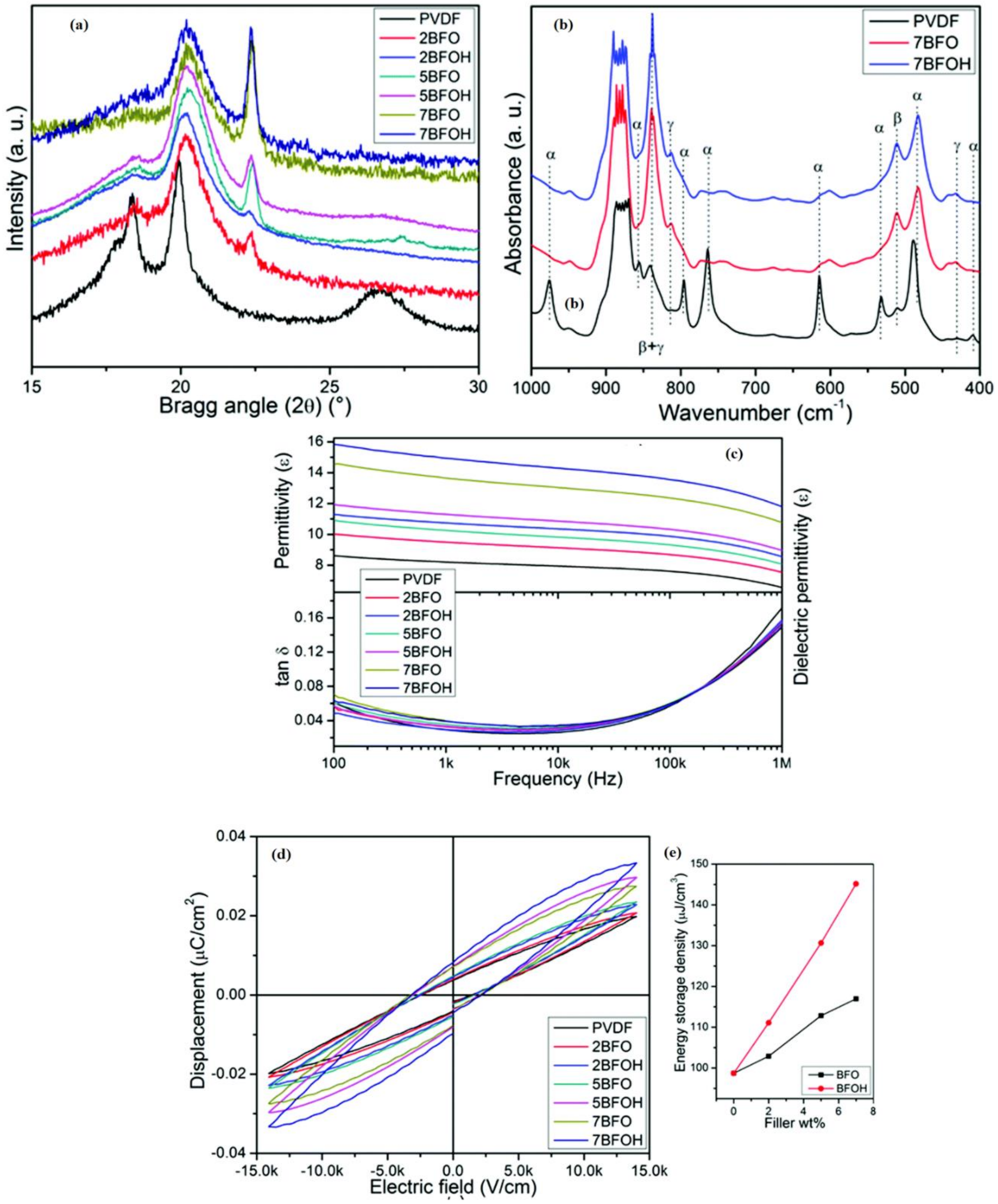

Figure 1.24 (a) XRD pattern, (b) FTIR analysis (c) Dielectric constant, (d) PE loop (e) Discharged Energy density of the $BiFeO_3$/PVDF [73].

Titanium carbide (TiC) filler in the PVDF matrix was used by the Wang et al. [74]. TiC fillers are thermally stable, erode-resistant, conducting, and inert to oxide formation. 11.58 vol% loading of the TiC in PVDF Matrix enhanced the dielectric constants to 540 and 150 at 100 Hz and 1 kHz respectively. The conducting and heterogenous nature of the TiC is responsible for the interfacial polarization resulting in high dielectric constant at low-frequency dielectric dependency. The enhancement in the dielectric properties is shown in the Figure 1.25.

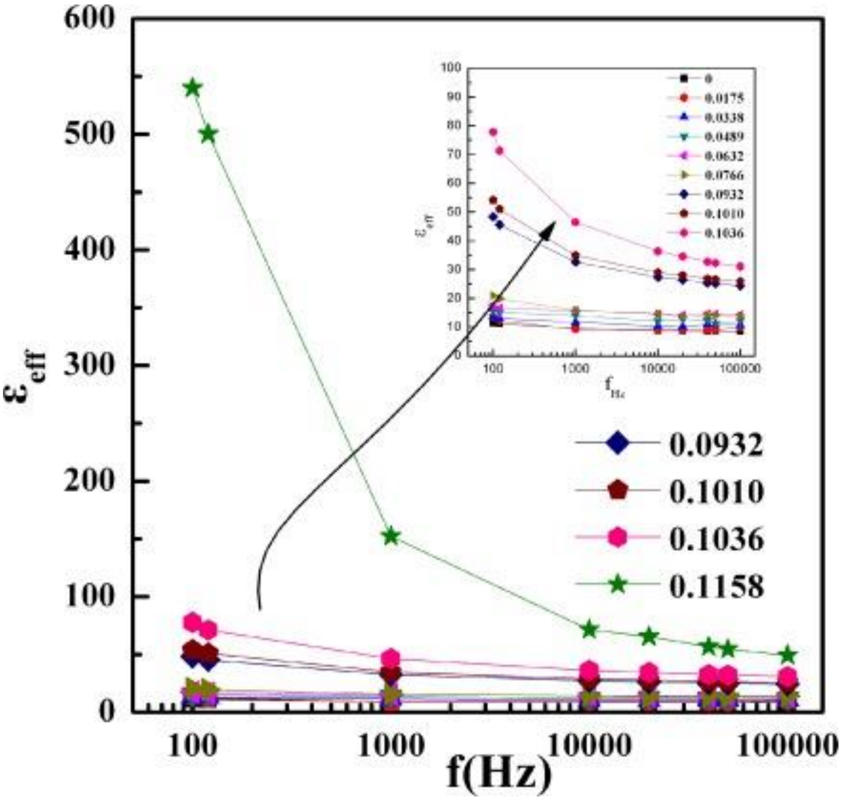

Figure 1.25 Dielectric constant of The TiC/PVDF (Inset) dielectric loss of the TiC/PVDF [74].

Other fillers like $CaCu_3Ti_4O_{12}$ have a very high dielectric properties (ε=2500 at 10 kHz) and shows no negative impact on the environment. Thomas et al. [75] synthesized the $CaCu_3Ti_4O_{12}$ fillers by solid-state reaction. The large amount of loading like 55 vol% of $CaCu_3Ti_4O_{12}$ in PVDF enhanced the dielectric constant to 80 and dielectric loss was around at 0.11 at the 1kHZ frequency. Dielectric constant rose with temperature, reaching 190 at 100 Hz at 150 °C, but declined to 65 at higher frequencies (100 kHz to1 MHz). The theoretical models (EMT and Yamada) were accurately satisfied the at the high loading of the filler in the PVDF. But Thomas et al. prepared the PVDF/$CaCu_3Ti_4O_{12}$ nanocomposites utilising the oxalate precursor synthesis process. Due to increasing polarisation among densely packed dipoles, the dielectric constant was enhanced from 18 to 70 at the frequency of 1kHz of the electric field when the $CaCu_3Ti_4O_{12}$ loading from 0 to 30%. Inhomogeneous conduction increased the leakage ($\tan\delta=0.15$ at 1 kHz) at 30% loading. $CaCu_3Ti_4O_{12}$ reinforced in the PVDF nanocomposites synthesized by the solid-state method shows greater dielectric characteristics than those synthesised from oxalate precursors.

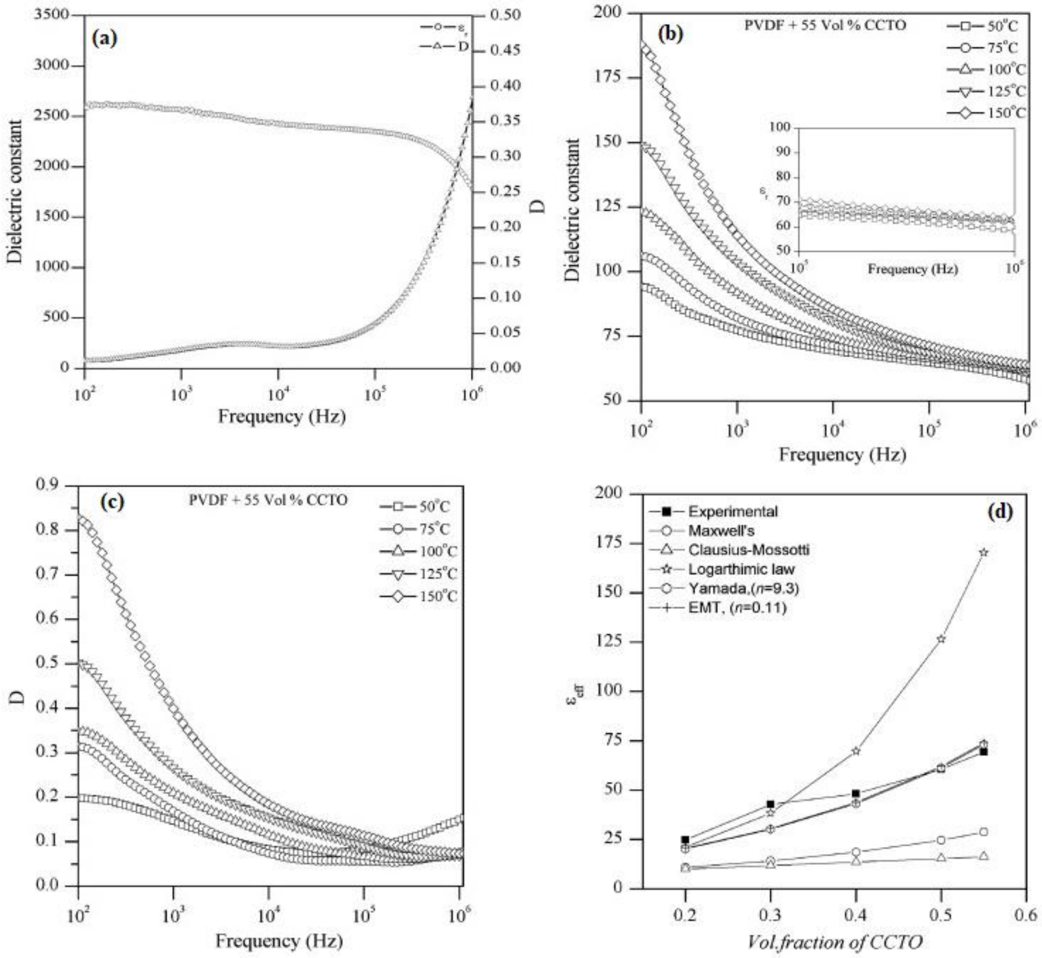

Figure 1.26 (a) Dielectric constant of the CCTO (solid solution)/PVDF, (b) Dielectric constant of the CCTO (Oxalate precursor)/PVDF and (c) Dielectric loss of the CCTO (Oxalate precursor)/PVDF, (d) Theoretical model fitting [75].

Chen et al. [76] prepared a unique system to enhance the storage properties of the PVDF based nanocomposite. The synthesized filler has co-filler having the Graphene quantum dots (GQDs) on the surface of the cobalt ferrite (CFO) to modify its surface properties. The GQDs are semiconducting in the nature whereas the CFO is low conducting with the magnetic properties. The GQD-CFO was reinforced in the PVDF as filler resulting in ternary nanocomposite. The fillers reinforced in the PVDF matric transformed the PVDF from nonpolar to polar phase. The enhancement in the dielectric properties of the PVDF nanocomposite was significant, the dielectric constant of the PVDF nanocomposite film was recorded at 1k Hz was more than 30 as compared to the pure PVDF (7.5). The dielectric properties enhanced are shown in the Figure 1.27.

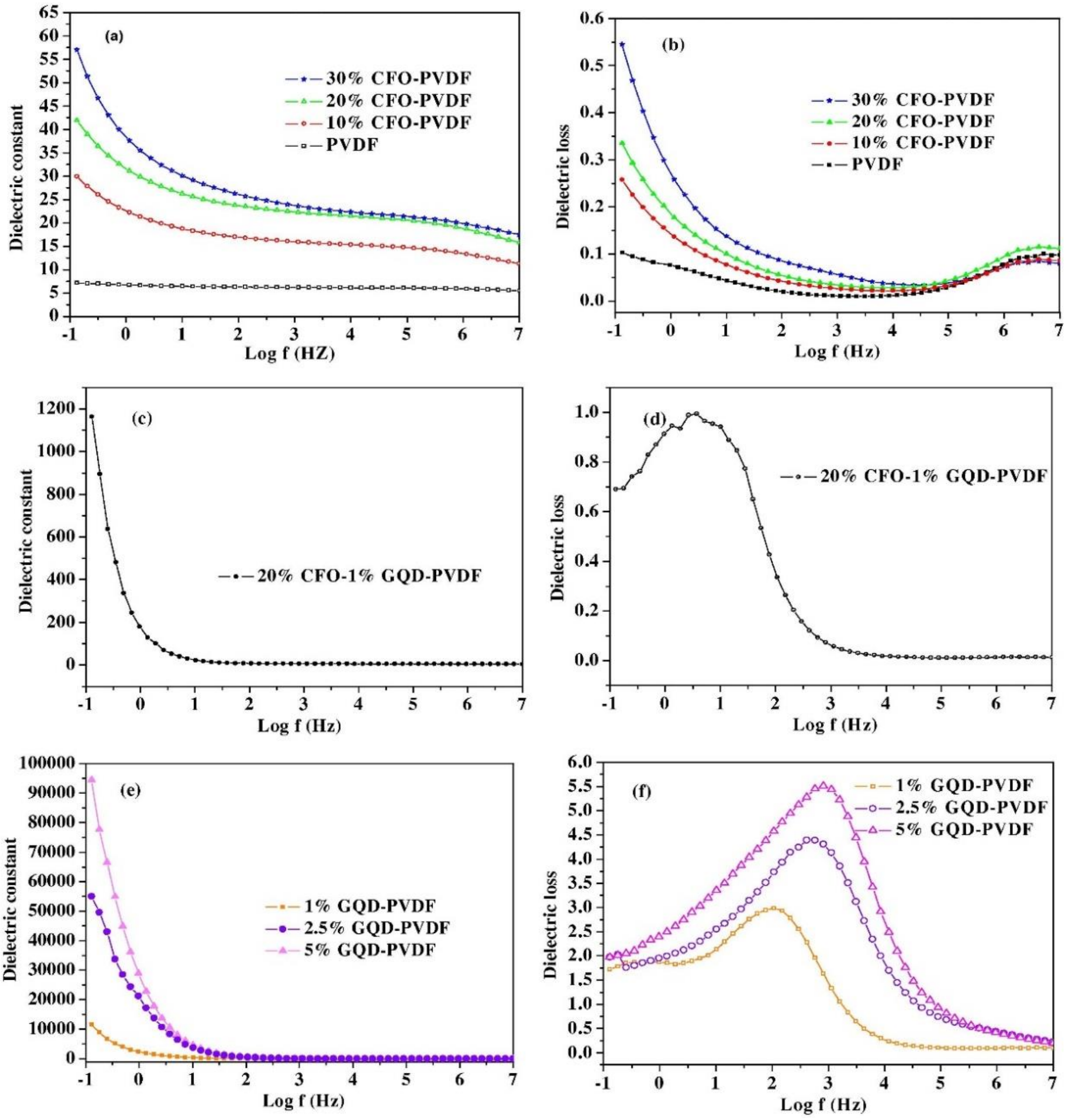

Figure 1.27 (a) Dielectric constant, (b) dielectric loss of PVDF and CFO reinforced PVDF. (c) Dielectric constant and (d) dielectric loss of 20%CFO-1%GQD reinforced in PVDF composite with frequency. (e) Dielectric constant and (f) dielectric loss of GQD reinforced in PVDF composites [76].

The space charge polarization played an important role in enhancement of the dielectric properties due to the interaction of the functional group present in the GQDs with the H and F atoms of the PVDF. The functional groups of the GQDs are C=O, C-O which helped in enhancement of the electroactive phase.

Chen et. al. [77] demonstrates a straight forward, and affordable solution casting synthesis process for developing the PVDF nanocomposite reinforced with 1D nano-conducting filler that is made up of natural sepiolite as the nanofiber core and conducting polypyrole as the nanofiber shell. The conducting polymer PPy (polypyrole) was oxidatively polymerized and doped with tiny molecules to get the 1D core-shell nanofiber (NF). The structural studies with the help of the XRD and FTIR shows that the PPy@Sep/PVDF nanocomposites have demonstrated electroactive phase causing ferroelectricity. PPy@Sep as filler is acting as a heterogeneous nucleating agent in PVDF and increases the crystallinity of the system with the loading below 3vol% of the filler. With increasing the filler content from 0 to 5 vol%, The enhancement in the dielectric constant is from 9 to 40 at 100 Hz, this enhancement can be attributed to the interfacial polarization and micro capacitor developed inside the nanocomposite film. This work inspires the fabrication of high-performance dielectric materials for microelectronics and soft actuators. Energy storage enhancement with the dielectric properties has been shown in the Figure 1.27.

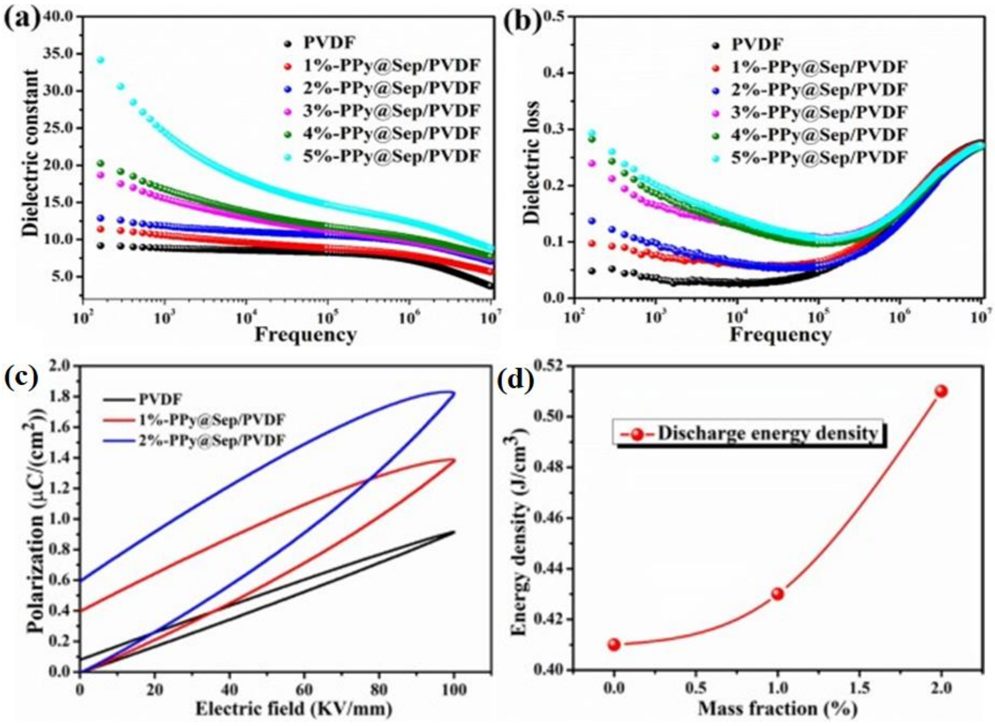

Figure 1.27 (a) Dielectric Constant, (b) Dielectric loss, (c) P-E loop, (d) Energy density of PVDF and Nanocomposite films.

1.7 Application of PVDF based Nanocomposite films

Polymer with filler ceramics, carbon materials, or conductive metals/or semiconducting materials, 2D Materials can increase energy storage properties and mechanical properties of polymer nanocomposites. Further modification of fillers and/or polymer matrices can enhance dielectric characteristics of nanocomposites. Enhancement in the energy density open the various applications. In this study, it can be concluded that polymer nanocomposite film dielectrics can be used in tiny energy storage or sensing devices, such as polymer film capacitors, flexible devices and wearable medical devices. To attain high energy density with good efficiency, structural properties, storage properties and dielectric characteristics must be explored in detail. The Figure 1.28 shows the applications of the nanocomposite films in various domains of the electronic devices.

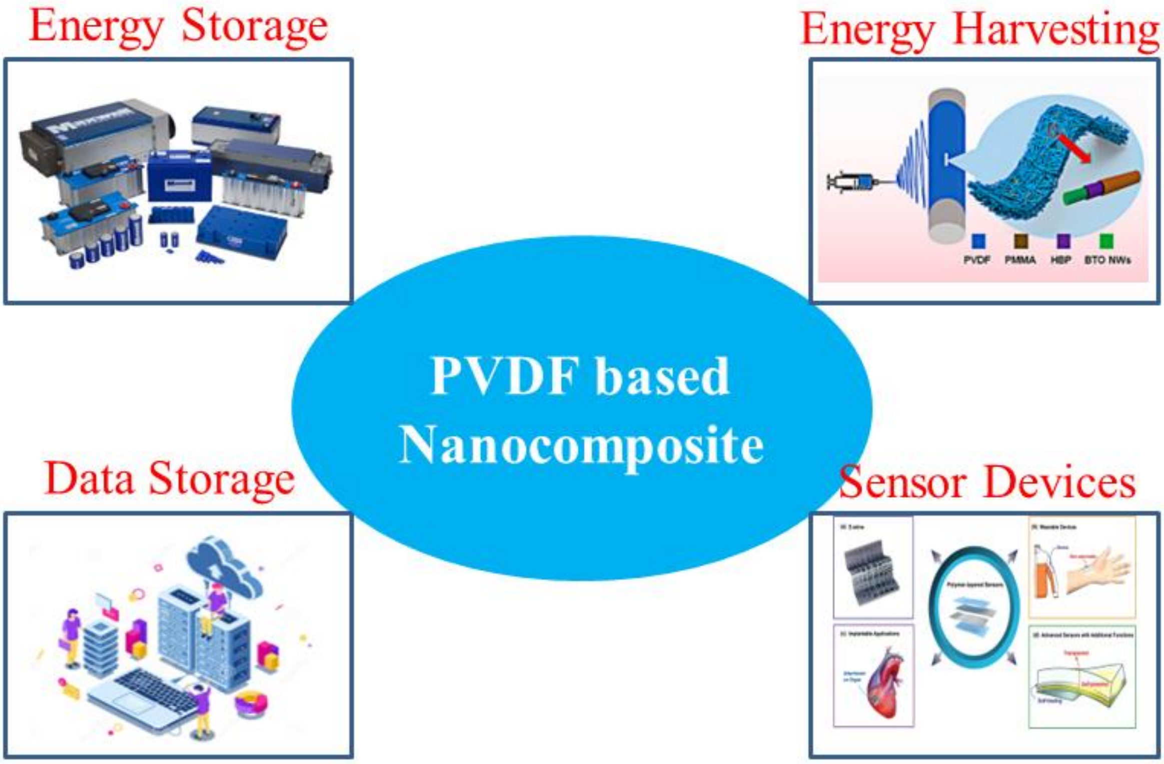

Figure 1.28 Application of the PVDF based Nanocomposite.

1.8 Motivation of the thesis

The primary encouragement behind the present research work was to explore the behaviour of the PVDF matrix with low amount of the different kind of semiconducting nanoparticles as reinforcement. We synthesized the 4 types of the nanocomposite film with varying composition of the filler in the PVDF Matrix, the filler was having different materials and structures. The conducting inorganic nanofiller particles were hydroxylated with the 30 vol% of the H_2O_2. Further, we synthesized the Nitrogen doped carbon dots, semiconducting in nature have been reinforced in the PVDF matrix. We were motivated to study the structural, morphological properties. The main motivation of doing this work was to develop a high energy density storage capacitor for the various electronic applications. For this, we studied the electrical properties in details. The dielectric properties and storage properties based on the experiments are studied and described in detail. To know the applicability of the developed films we have measured the Polarization vs electric field hysteresis loop and have calculated the energy density for all the compositions. The visualization is done with the help of the COMSOL Multiphysics software 5.5 what is going inside the film and how the electric field, space charge density is behaving with the nanoparticles of inside PVDF matrix.

1.9 Objective of the present work

A we have already discussed in literature review, PVDF matrix has been reinforced with the dielectric ceramic ($BaTiO_3$, $SrTiO_3$, $BaZr_{1-x}Ti_xO_2$ ($0<x<1$) etc.), semiconducting materials (Carbon black, TiO_2 etc) to enhance the desired storage properties.

The summarized objective of the work is given below:

1. To investigate the selection of the suitable semiconducting nanofiller to reinforce in PVDF matrix.
2. The study of the different semiconducting filler and modification of the PVDF nanocomposite to prepare superior, economic dielectric flexible films for high energy density storage
3. To study the influence of all chosen semiconducting fillers on dielectric properties of the including breakdown strength of PVDF nanocomposites.
4. To study the electric breakdown strength and interfacial polarization importance in achieving high energy density of the nanocomposite film for the application in high energy voltage.
5. To study the polarization and dielectric loss mechanisms in PVDF nanocomposite films to get large polarization and low loss for high energy density energy storage application.

The main objective of the present thesis work is following:

1. To develop and understand the storage and ferroelectric properties of Hydroxylated V_2O_5 reinforcement in the PVDF matrix for the flexible nanocomposite film.
2. To develop and understand the Poly (vinylidene fluoride)/Nitrogen doped carbon dots nanocomposite film with improved storage properties for high energy density applications.
3. To develop and understand the Poly (vinylidene fluoride)/ hydrated antimony pentoxide (HAP) based nanocomposite film for high energy density applications.
4. To develop and understand the H_2O_2 Hydroxylated Rare earth (La, Gd) FeO_3 nanoparticles loaded as Filler in PVDF nanocomposite film for the high energy density energy storage applications.